ABSTRACT

DESTRUCTIVE DISASSEMBLY OF BOLTS AND SCREWS USING IMPACT

by

Kyung Geun Pak

Disassembly, the process of separating parts or components at the end of their useful life is complex due to a variety of fastener shapes and variability in their damage during use. As a natural solution, mechanical impact has been suggested as a cost-effective method for destructive disassembly of joining elements.

The objective of this research is to improve the efficiency of impact disassembly process by studying the characteristics of elastic waves caused by impact. This research presents a new method for increasing the shear stress applied on the bolt head without increasing the energy input invested on launching striker. The equations are developed for the elastic waves in one-dimensional bar that transfers the impact energy to a protruded bolt head mounted on an infinite elastic medium or structure. These equations represent the stress wave for each period when the stress wave caused by impact travels back and forth between the struck end and the other end that is in contact with the bolt head mounted on an elastic body. The equations determine the impact load exerted on the bolt head and also the impact force generated to shear-off the bolt head.

Since these equations are developed based on the assumption that the stress waves reflect at the bolt-contacting surface with a constant ratio, the reflection characteristics significantly affect the precision of the analysis.

The reflection characteristics from a bolt head are found to be more complex than expected, and they affected the experimental result deviate from the analytical result.

However, the analysis and the experiment on relative evaluation between the developed method and the conventional method show that the energy efficiency is improved with the developed method.

The results can be used to design effective destructive disassembly procedures for recycling processes and to develop new destructive disassembly devices for removing bolt or screw fasteners. This research has potential for advancing de-manufacturing technology resulting in an increase of disassembly efficiency and reducing recycling cost.

DESTRUCTIVE DISASSEMBLY OF BOLTS AND SCREWS USING IMPACT

by
Kyung Geun Pak

A Dissertation
Submitted to the Faculty of
New Jersey Institute of Technology
in Partial Fulfillment of the Requirement for the Degree of
Doctor of Philosophy in Mechanical Engineering

Department of Mechanical Engineering

May 2002

APPROVAL PAGE

DESTRUCTIVE DISASSEMBLY OF BOLTS AND SCREWS USING IMPACT

Kyung Geun Pak

5/9/02

Dr. Raj S. Sodhi, Dissertation Advisor — Date
Associate Professor of Mechanical Engineering, NJIT

5/9/02

Dr. Reggie J. Caudill, Committee Member — Date
Professor of Industrial and Manufacturing Engineering and Executive Director,
Multi-lifecycle Engineering Research Center, NJIT

5/9/02

Dr. Rong-Yaw Chen — Date
Professor of Mechanical Engineering, NJIT

5/9/02

Dr. Sanchoy K. Das, Committee Member — Date
Professor of Industrial and Manufacturing Engineering, NJIT

5/9/02

Dr. Pushpendra Singh — Date
Associate Professor of Mechanical Engineering, NJIT

BIOGRAPHICAL SKETCH

Author: Kyung Geun Pak

Degree: Doctor of Philosophy

Date: March 2002

Date of Birth:

Place of Birth:

Undergraduate and Graduate Education:

- Doctor of Philosophy in Mechanical Engineering,
  New Jersey Institute of Technology, Newark, NJ, 2002

- Master of Science in Mechanical Engineering,
  New Jersey Institute of Technology, Newark, NJ, 1990

- Bachelor of Science in Mechanical Engineering,
  Han Yang University, Seoul, Korea, 1988

Major: Mechanical Engineering

Presentations and Publications:

Kyung G. Pak and Raj S. Sodhi,

"Destructive Disassembly of Bolts and Screws by Impact Fracture,"
Accepted to the Journal of Manufacturing Systems,
October, 2001.

Kyung G. Pak and Raj S. Sodhi,

"Analytical and Experimental Investigation on Destructive Disassembly of Bolts and Screws using Mechanical Impact,"
Submitted to the Journal of Manufacturing Systems,
February, 2002.

Kyung G. Pak and Raj S. Sodhi

"Destructive Disassembly of Bolts and Screws using Mechanical Impact,"
Accepted for presentation to the 14th U.S. National Congress of Applied Mechanics, Blacksburg, VA. January, 2002.

To my family

ACKNOWLEDGMENT

The author would like to express his sincere gratitude to Dr. Raj S. Sodhi for his service, resources, advice and support through this research. Special thanks to Dr. Reggie J. Caudill, Dr. Rong-Yaw Chen, Dr. Sanchoy K. Das and Dr. Pushpendra Singh for serving as committee members. The author is also grateful to the Department of Mechanical Engineering of New Jersey Institute of Technology for the financial support throughout the program. The author appreciates Mr. Joe Glaz, Laboratory/Technical Coordinator, for his timely help, provisions and suggestions to perform experiments.

The author wishes to thank his lovely wife, Sunhee, for her unconditional support and encouragement, and to his mother in law for the financial support of him and his family. Finally, the author wishes to thank the vast majority of unnamed supporters, both great and small, helped make this work possible.

TABLE OF CONTENTS

Chapter		Page
1	INTRODUCTION	1
	1.1 Destructive Approaches in Product Disassembly	2
	1.2 Research Objectives	3
	1.3 Research Approach	4
2	DISASSEMBLY IN DE-MANUFACTURING	6
	2.1 Researches in De-manufacturing	6
	2.2 Methods for De-manufacturing	10
	2.3 Destructive Disassembly for End-of-Life Products	14
3	IMPACT MECHANICS IN DESTRUCTIVE DISASSEMBLY	20
	3.1 Introduction	20
	3.2 SRSW Method	21
	3.3 MRSW Method	24
	3.3.1 Determination of l_t to Apply MRSW Method	26
	3.3.2 Efficiency of MRSW Method	27
4	EQUATIONS FOR STRESS WAVES IN A BAR CAUSED BY IMPACT	28
	4.1 Stress Wave Equations when Bolt is Mounted on a Rigid Body	28
	4.2 Stress Wave Equations when Bolt is Mounted on an Elastic Body	31
	4.3 Determining the Reflection Ratio R	38
	4.4 Increase in Maximum Stress by MRSW Method	40
5	EXPERIMENTAL INVESTIGATION	42
	5.1 Experimental Setup	42
	5.1.1 Setup for Measuring the Reflection Characteristics of Stress Wave	42

TABLE OF CONTENTS
(Continued)

Chapter **Page**

5.1.2 Setup for Measuring Stress Wave Profile 45

5.2 Reflection Characteristics of Stress Waves 47

5.2.1 Experimental Results 47

5.2.2 Determining Reflection Ratio *R* 50

5.3 Numerical Analysis and Experimental Results 52

5.3.1 Stress Profile at the Bolt-Contacting End with SRSW Method 52

5.3.2 Stress Profile at the Bolt-Contacting End with MRSW Method 54

5.3.3 Increase in Maximum Stress by MRSW Method 56

5.4 Applying Impact on a Smaller Bolt Head 57

5.4.1 Experimental Setup 58

5.4.2 Reflection Characteristics from a Smaller Bolt Head 58

5.4.3 Stress Wave Profiles with a Smaller Bolt Head 60

5.4.4 Efficiency of MRSW Method with a Smaller Bolt Head 63

6 DISCUSSION AND APPLICATION IN PRODUCT DISASSEMBLY 64

6.1 Discrepancies between Analysis and Experiment 65

6.1.1 Positioning Problem of Strain Gauges 65

6.1.2 Contact Condition between Transmitter Bar and Bolt Head 68

6.1.3 Elasticity of Striker 70

6.1.4 Damping Effect of Transmitter Bar 70

6.1.5 Non-Constant Characteristics of Reflection Ratio *R* 71

6.1.6 Extension of Time Intervals between the Peaks 72

TABLE OF CONTENTS
(Continued)

Chapter		Page
	6.2 Application of MRSW Method in Destructive Disassembly	73
7	CONCLUSIONS AND RECOMMENDATIONS FOR FUTURE WORK	75
	7.1 Contribution to Destructive Disassembly	75
	7.2 Recommendations for Future Work	77
APPENDIX		79
REFERENCES		83

LIST OF TABLES

Table **Page**

4.1 Increase in Maximum Stress for Different Reflection Values (For $\alpha = 0.25$)..... 40

5.1 Sizes of Bolt and Beams in the Assembly..... 44

LIST OF FIGURES

Figure		Page
2.1	Integrated tools for the transmission of forces and torques	16
2.2	Side impact for destructive disassembly	18
3.1	Single reflection of stress wave from a rigid bolt head	23
3.2	Multiple reflection of stress wave from a rigid bolt	25
4.1	Schematic of instrument setup for impact fracture of bolt	28
4.2	Reflection and dissipation of compressive stress wave from a bolt mounted on an elastic medium	32
4.3	Stress ratio σ/σ_0 at struck end for different R-values	35
4.4	Stress at bolt-contacting end for different values of R ($\alpha = 1/4$)	36
4.5	Maximum stress at bolt-contacting end for different values of mass ratio	37
5.1	Setup for measuring reflection of stress waves	43
5.2	Angled beam assembly	44
5.3	Experimental setup for Measuring Stress Wave Profile	45
5.4	Reflection of stress wave from a bolt head	47
5.5	Transmitter is in contact with an edge of the angled beam assembly	48
5.6	Reflection of stress wave from an edge of the angled beam assembly	49
5.7	Reflection of stress wave from a bolt head (striker length = 338mm)	50
5.8	Incident pulse from equation (4.1) and its experimental result	52
5.9	Stress at bolt-contacting end (SRSW)	54
5.10	Stress at bolt-contacting end (MRSW)	55
5.11	Stress profiles near bolt contacting end (Experimental result)	56

LIST OF FIGURES
(Continued)

Figure **Page**

5.12 Contacting surface area is reduced in half with smaller bolt head 58

5.13 Reflection of stress wave from a smaller bolt head 59

5.14 Stress at bolt-contacting end with smaller bolt head (SRSW Method) 60

5.15 Stress at bolt-contacting end with smaller bolt head (MRSW Method) 61

5.16 Stress at bolt-contacting end with larger bolt head (MRSW Method) 62

6.1 Delay in stress wave superposition due to the positioning problem of strain gauges 65

6.2 Graphic illustration of delay in stress superposition 66

6.3 Higher and longer tensile peaks due to a poor initial contact 68

6.4 Lower and shorter tensile peaks due to a better initial contact 69

6.5 Reflection of stress wave showing constant reflection magnitude 71

6.6 Experimental result of MRSW Method showing irregularity in time intervals between the peaks 72

A.1 Experimental setup 79

A.2 Pen plotter, HP4470A 80

A.3 Oscilloscope, Tektronix 2230 80

A.4 Bridge box and strain amplifier, VISHAY ELLIS-20 81

A.5 Transmitter for measuring reflection characteristics and striker 81

A.6 Striker hitting transmitter in SRSW Method 82

A.7 Striker hitting transmitter in MRSW Method 82

CHAPTER 1

INTRODUCTION

Unlike the assembly process, disassembly process of products at the end of a life cycle is generally manual and involves complex problems. The process is especially difficult when dealing with a large variety of products and uncertainty in product condition or damage after use. The aim of the disassembly process should be cost minimization, hazardous materials isolation, and opportunities to re-use or re-utilize materials and components. Therefore, an appropriate disassembly technology must combine flexibility and robustness to be able to deal with these issues. The disassembly process involves three activities: i) unfastening to separate the components, ii) the destructive disassembly where either the fastener and/or the component may be destroyed and iii) the partly destructive or semi-destructive disassembly where the fastener can be destroyed during the disassembly process with no damage to the components. The efficiency of the disassembly process is presently not well understood especially for destructive methods such as cutting, sawing, or breaking the joining elements e.g. screws and bolts. Since the efficiency in recycling is an important issue, there have been some recent researches on destructive disassembly techniques. In general, a product is a combination of parts or subassemblies assembled by joining elements. Therefore, determining the effort needed to disassemble these joining elements has become a vital issue in de-manufacturing research.

1.1 Destructive Approaches in Product Disassembly

The purpose of product disassembly determines the procedure of disassembly and the methods involved in each process. When a product is disassembled for service or maintenance, the disassembly process should be reversible, so that the product can be used as it is originally designed. In general, the disassembly processes for service follow the inverse of assembly operation or other relatively simple processes. However, when a product is disassembled for recycling purposes at the end of its life cycle, there are many options for disassembly procedure and many more issues to consider than dealing with newly assembled products. Such options and issues include disassembly methodology, logistics problems, environmental concerns, security issues, legal liability, indemnification, financial analysis problems and etc. Therefore, the disassembly process becomes more complex and it demands a new technology that would deal with these issues effectively. The destructive approaches in product disassembly are widely accepted as recycling purposes for its economical advantages and robustness.

In several disassembly line situations with the wide range of fastener geometry and variation in fastener damage during use, it is advantageous to destroy the fastener element to achieve economic viability of the process. Therefore in this study, the research takes the destructive approach and focuses on developing a robust method for breaking protruded head of joining elements such as screws and bolts by applying side impact. Specifically, the analytical equations are derived to represent the impact stress in a transmitter bar and the shear stress in the bolt head mounted on an elastic medium. Based on the developed equations and the experiments, the efficiency of the developed method in comparison with a conventional method is evaluated. The presented

research should lead to an accurate determination of destructive disassembly effort of commonly used fasteners and subsequently assist in developing an efficient destructive disassembly procedure.

1.2 Research Objectives

The overall mission and objective of this research is to develop a new method, which will improve the efficiency of destructive process for breaking protruded head of joining elements by applying side impact. The analysis and the experimental tests performed in this research will provide information needed to understand the impact mechanism involved in the destructive disassembly process. Using this analysis, a new method will be developed that creates higher maximum shear stress at the neck of joining element without increasing the energy invested in launching striker. As discussed in the literature review (Chapter 2), current researches do not address the theoretical aspects of stress waves in one-dimensional bars used for transmitting impact energy to bolt head. Therefore, the overall goal of this research is to investigate theoretically and experimentally the mechanism involved in applying side impact on a protruded joining element, and to develop a new method that will improve the efficiency of the destructive disassembly process. More specifically, this research will:

1. Develop the equations representing stress waves in one-dimensional bar caused by impact when the bar is in contact with a bolt head mounted on an elastic medium.
2. Develop the equations for the shear stress at the bolt neck from the equations of stress waves. These equations will be developed for both cases of single reflection and multiple reflections.

3. Develop a new method that generates higher shear stress at the neck of joining element without increasing the energy input to striker. A comparison between the results from analytic equations of developed method and conventional method will be presented.

4. Provide the experimental results that show the reflection characteristics of stress waves from a bolt head and the profiles of stress waves generated by developed method and conventional method. The experiments will prove the feasibility of the developed method.

5. Evaluate the efficiency of the developed method in comparison with the conventional method.

1.3 Research Approach

The approach taken to meet the objectives of this research is to:

1. Model the mechanical arrangement that is commonly used for applying mechanical impact to a protruded head of joining element. Based on this model, the equations of stress waves at the struck end will be derived for each period while the front end of stress wave travels back and forth between the struck end and the other end that is in contact with the head of joining element.

2. Transform the derived equations in Step 1 to the equations representing the stress at the surface contacting with the head of joining element. These equations will be converted to derive the equation for shear stress at the neck of joining element. The derived equation for shear stress is useful in practical implementation. However, the research focus will be on the stress at the surface contacting with the

head of joining element.

3. Calculate and compare the maximum stresses at the surface contacting with the head of joining element. The comparison will be made between the maximum stresses acquired using the developed equations for the cases of single and multiple reflections of stress waves.

4. Conduct experiments to find out the reflection characteristics of stress waves from a protruded head of joining element mounted on an elastic body. The experiments will be conducted to record the stress profiles near the joining element by applying the conventional method and the developed methods.

5. Compare the experimental results to the analytic results and evaluate the factors that cause discrepancies between them. The comparison also will be made between the experimental results acquired by applying conventional method and the developed method. The feasibility of new method will be demonstrated by showing the increase of maximum stress.

CHAPTER 2

DISASSEMBLY IN DE-MANUFACTURING

2.1 Researches in De-manufacturing

Researches on disassembly are relatively recent activities. Because of demand from consumer and new regulations from government, manufacturers are required to reduce the quantities of manufacturing waste they generated or reclaim responsibility for their product at the end of product life cycle. Consequently, a firm's competitiveness in future world markets depends upon making environmental issues a central concern [1]. Recently, researchers have begun to address and devise general and standard solutions for many aspects of product disassembly. Since disassembly is a necessary and critical process for all end-of-life products, there have been many researches in how to design products for easier disassembly. Much of this research emphasizes disassembly to facilitate recycling [2][3][4][5]. There have been many researches on the design for disassembly (DFD), which involves the development of products that are easy to take apart to enable recycling. Research related to DFD has increased in recent years but a major thrust of the work on disassembly has been focused on disassembly sequencing, disassembly path planning, and the evaluation tool development. Gupta [6] and Penev [7] have provided and overview of the ongoing research in disassembly and the trends for future activities. Hrinyak [8] has examined the existing disassembly software tools presently available to the designers. Recently, Shyamsunder and his associates [9] have initiated work to build a three-dimensional virtual disassembly tool.

In order to find a method that evaluates a product's environmental consequences, Life Cycle Assessment (LCA) methods have been researched extensively in recent years

[10][11][12]. Vigon and Curran [13], Tummala and Koenig [14] and, Veldstra and Bouwa [15] are the major studies related to LCA. These studies describe LCA as a systematic procedure to evaluate energy use, raw material consumption and waste emissions during the complete cycle of a product. The use of this procedure necessitates the determination of extensive data regarding product's manufacture and disposal. Though LCA studies have been popular in Japan, its use as a design tool is unlikely until simpler procedures and accurate life cycle databases are developed (Hanft and Kroll, [16]).

Another similar procedure called Activity Based Approach (ABC) has been proposed by Emblemsvag and Bras [17]. This method is based on assessment of the consumption of activities rather than energy or raw material. According to this approach, all the operations associated with the remanufacture of a product are considered as a single activity. Therefore, the product's cost is the sum of the costs of all the processes performed on it during its life cycle. Using design parameters, the procedure calculates alternative design metrics and compares associated activity costs. The method has both advantages and disadvantages. It is easier for engineers to obtain de-manufacturing costs in terms of dollars rather than energy expanded as in LCA method. Zussman et al. [18] have determined the optimum end-of-life scenario for a product. They use probability density functions for evaluation criteria of future conditions through forecasts by experts. Issues such as future labor costs and expected lifetimes of products are approximated with the forecasts.

A more recent procedure for the recovery analysis of products has been developed by Navin Candra [19]. This is a computer-aided design tool for recovery analysis of products where the disassembly planning and optimization program is based on a

decision tree. The designer inputs information as to the type of fasteners and the constraints used and subsequently determines the most profitable de-manufacturing scenario using a data and times. Hanft and Kroll [16], have presented a procedure for evaluating Ease-of-Assembly for product de-manufacturing. They use a spreadsheet like disassembly sequences for the same product with focus on manual disassembly of business equipment. The method provides a means for identifying design weaknesses and comparing alternatives. The authors indicate a need to develop similar procedures for automated disassembly of products, which they claim to be a challenging task due to unequal wear in each product, the variety of disassembly processes and the flexibility in parts such as wires.

Masataka Yoshimura [20] has presented a design optimization strategy for designing products for the complete life cycle. Product life cycle based on the environment of a product is classified into three categories, which focuses on "manufacturing products", "selling products" and "using products". After comprehending the environments of the products, concurrent processing of information and knowledge related to the product decision making is conducted so that the product design satisfies the requirements of the scoring scheme to quantify the degree of difficulty of disassembly of various fasteners. They have integrated all the disassembly information into a CAD database. Their database is applicable to specific products such as PC's. It needs to be expanded to be more generic and applicable to other products.

Most of the researches related to disassembly for recycling are to find a model to compute the disassembly effort and to facilitate the economic analysis of the disassembly activities. Das, Yedlarajiah and Narendra [21] introduced a methodology that support and facilitate the economic analysis of disassembly activities. They presented a multi-

factor model to compute the disassembly effort index (DEI) score, which is representative of the total operating cost to disassemble a product. The DEI score can then be compared against the projected market value of the disassembled parts and subassemblies to get an economic measure. Based on the survey of various commercial disassembly facilities, they have developed a multi-factor weighted estimation scheme. These factors include: time, tools, fixture, accessibility, instruction availability, hazard, and force requirement. The DEI scale, which is defined in the 0 to 100 ranges, is assigned on a weighted basis to each of these factors. Then for each factor, an independent utility scale is formulated using the assigned range as anchors. Using a conversion scale, the DEI score is used to derive an estimate of disassembly cost and the disassembly return on investment.

Knight and Boothroyd [22] analyzed disassembly activities in terms of financial and environmental aspects. They presented methods for optimizing disassembly sequences to release valuable or environmentally beneficial items as early possible. In an effort to standardize disassembly operation times, Dowie and Kelly [23] conducted a series of disassembly experiments with simple operations including destructive operations. They recorded times for a wide variety of operations, including screw removal, cutting, and snap-fit release. Kroll [24] and Kroll et al [25] developed a method for estimating the ease of disassembly using work measurement analysis. Hanft and Kroll [16] proposed a metric for evaluating disassembly activities such as: drilling, sawing, grinding and proposed a metric for evaluation. Other work extends to include disassembly for maintenance [26][27][28][29] as well as remanufacture [18]. The primary emphasis in disassembly is to minimize machine downtime and maintenance labor cost.

Seliger, Hentschel and Wagner [30] reported several research projects including design of new tools for disassembly, logistics, product evaluation and disassembly planning, and design for disassembly. Among the examples of research proposals, they presented a disassembly tool that create acting surfaces during the disassembly process using impact stamping of screw head surface with impulse forces. Since this disassembly tool creates new acting surface before transmitting forces and torques, the end-effector become independent of the acting surfaces that already exist in the joining element and is robust against uncertain conditions like corrosion or others. Therefore, the disassembly processes would become cost-effective with a reduced number of tools and time-consuming tool changes. One other research project they presented, uses fuzzy theory [31] for the disassembly and recycling planning of end-of-life products. With this new approach for grouping, important disassembly and recycling information can be derived and characterized from the products' design attributes such as: the country of origin, the size and the weight of the product, usage condition and etc. This new approach is suggested based on fuzzy set theory to cope with a high level of uncertainty on the products' characteristics after use [32].

2.2 Methods for De-manufacturing

De-manufactured objects are influenced by different factors like volume or weight of the structure, the number of parts, accessibility, arrangement, freedom of movement, wear, corrosion, ability to clamp, complexity, sensitivity, and expenditure for cleaning. The processes in de-manufacturing can be divided into two groups: non-destructive and destructive. Non-destructive methods are used for soluble connections like assembled, filled, pressed against and presses in connection, and destructive methods for insoluble

ones like welding, adhesive, rivet or soldering joints. Deformed and textile connections can belong to both groups. With that, the functionality will be lost. Non-destructive methods are usually time-consuming disassembly methods, because the components are de-manufactured reverse order. Between these two groups, there exists a transition state of partly destructive methods, with which parts are not damaged, however, the fastener or fastening element will be destroyed. This is usually very advantageous, because the parts can be recovered and then reused. Further, with the partly destructive method the process can be accelerated, because the intended destruction of the fastening element usually needs less time than the reversed assembly process.

Based on a systematic approach according to DIN 8580, the process methods for the de-manufacturing can be classified in six different groups:

- To disassemble:

  Generally, these are non-destructive methods of separation without damage to the parts. In de-manufacturing, only the taking apart and the loosing are for the time being. The other methods (to empty, to melt-away, to form-away, to solder-away, to glue-away, to take textile away) are tried in experiments, however, until now they could not find use in the actual de-manufacturing processes. Somehow, it also can be difficult how far they are non-destructive.

- To separate:

  The characteristic of separation is the breaking of the material-fit connections. Hereby, four different methods can be distinguished: to cut into pieces, to split up, to tear, to break. In de-manufacturing process, mainly the cutting is used, because the other methods are more difficult to control.

- To cut:

  The cutting or machining in de-manufacturing and the cutting or machining in production are different. In the production, a part is produced through cutting of a raw part or material, whereby functional surfaces are created. In de-manufacturing, it is the goal to separate to basic assembly groups through the cutting of connection links without influencing the geometry of the parts or the functionality of the system. The cutting or machining can be divided into ten groups: to turn away, to drill away, to mill away, to slot away, to shape away, to broach away, to saw away, to file away, to chisel away, and to grind away. The problem of cutting in de-manufacturing is to present the difficulty with the fixing or holding of the part or system.

- To beam-cut:

  These are methods where the separation is the result of the use of a beam or a jet. It can be divided into four groups: to water jet cut, to laser beam cut, to plasma cut, to flame cut (torch cut). Because only small process forces are needed these are quite important methods in the de-manufacturing processes

- To de-melt:

  Here the connecting link is removed through melting. The solid area of the part becomes at this place liquid. Through this, the material-fit, form-fit or non-negative connection disappears. At least one part will be partly or totally damaged and destroyed. This method can be divided into three different groups: to melt away, to torch cut, to melt down.

- To deform:

  The separation is caused by deformation. This method destroys parts and causes final damage to the parts. It means the parts cannot be used again. This method can be distinguished into five different groups: to deform wire, to deform plates, to deform tubes, to deform profiles, to deform rivets.

For de-manufacturing, other conditions and quality criteria are relevant than for the standard production and assembly process. In the de-manufacturing the degree of separation, the functionality of the separated parts and the cost for the disassembly process are the main factors. Here the degree of separation depends on the cutting speed and if at the end the parts are completely separated or not. The functionality is a measure for the degree of damage during the disassembling process. If a part is mot damaged at all, then the degree of functionality is 100%. The costs depend on the machine cost per hour.

Some criteria to help eliminate unsuitable methods for the de-manufacturing process:

- Accessibility:

  Methods, which require accessibility from two sides, like rolling, are not suitable.

- Time:

  Methods that have only small changes per time unit, like electric erosion, are not proper for efficient de-manufacturing.

- Relative motion of object:

  Methods which need a movement or motion of the object, like turning, are not

appropriate methods because of the size of some de-manufacture objects.

Also, the limitation of physical effects for the transmission of forces can be critical. They include:

- Size:

  Principles where only small forces per area are created, like electric static, are not powerful enough for a de-manufacturing process.

- Material dependency:

  Principles that are bound to certain material properties of object, like magnesium, are not suitable because of the material variety of the old products.

- Additional work:

  Principles that need the direct contact of liquid or gaseous agents with the de-manufacturing object require extravagant gaskets or sealing, which cannot be accomplished if the geometry is quite complex.

2.3 Destructive Disassembly for End-of-Life Products

Although the overall economics of disassembly process is still not well understood, the destructive disassembly approach is adopted in many recycling processes for fast and efficient separation of products. Feldmann and Meedt [33] adopted use of destructive or partially destructive processes for efficient and flexible disassembly of electronic devices. They presented methods for the planning of optimal disassembly and the calculation of the most economic disassembly depth, and reported the need of highly flexible tools designed for disassembly operations. They proposed devices (drill-driver and drill-

gripper) that combine transmission of torques or forces with drilling for unscrewing various types of screwed fasteners and for increasing transmittable forces. The drill driver is a tool, similar to a left-turning twist drill with two cutting edges, which are shaped in a special geometry. Due to its special geometry, a drill-driver can perform transmission of torques either by using existing working points or by using self-created drill chips as starting points. Using a drill-driver, the following important disassembly functions can be fulfilled:

- For the fasteners like cross recessed screws, hexagon sockets, and other many screw types, this special geometry of the drill-driver allows to generate a form closure between the cutting edges on it and existing working points of these screws. Then this form closure is used to transmit the torque for unfastening.
- If there are no working points for form closures available, a short drill process is needed with the drill-driver to create drill chips, which are used afterwards to transmit the torque. Both processes, drilling and the transmission of the torque are done without tool change.
- The drill-driver can be used similar to a drill bit to remove material with high rotational speed until the joining is disassembled. When the disassembly of the joining element by transmission of torque is not possible, this function makes it possible to destroy joining elements such as corroded screws, rivets, and spot welding points.

They introduced the drill-driver as an extremely flexible device, concerning different fastener types and sizes as well as concerning different disassembly processes (non-destructive, partial destructive, or destructive).

One other device that they have developed and patented is a tool that integrates a drill and a grip device, and is called drill-gripper. As shown in Figure 2.1(a), a working

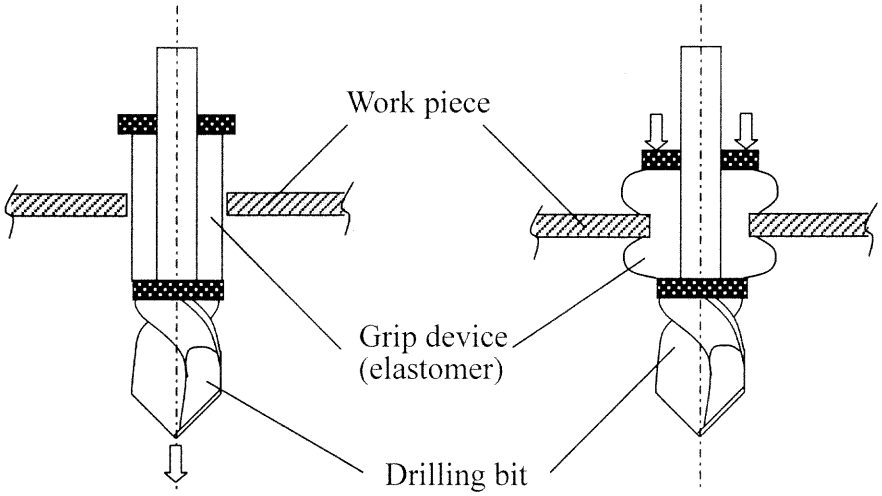

(a) Creating a working point by drilling.

(b) Activating the grip device by shortening an elastomer.

Figure 2.1 Integrated tools for the transmission of forces and torques.

point is created by drilling a hole in the product or component. Then the grip device is shortened by pressure and the diameter of the elastomer increases so that a form closure between the tool and the component is created. The grip process can be finished by elongating the grip device. By the use of this tool, the following operations are possible:

- Grip and clamp processes for handling and fixing complex products without existing usable working points.
- Transmission of high forces in order to achieve a destruction of components (i.e. housings).
- Many drill-grippers can be combined in order to increase the transmittable forces and

to transmit torques.

- With little changes the tool can be used for the continued transportation and handling of work pieces. In this case, the tool is fixed at the work-piece and is used as a defined working point for handling and transportation systems.

They also have proposed a device that combines the drill-driver and the drill-gripper so that the processes of "transmission of forces" and "transmission of torques" are integrated. Therefore, using this integrated flexible tool makes it possible to fulfill the requirements of many disassembly processes without tool change.

A very interesting disassembly method is presented by J.D. Chiodo, E.H. Billett and D.J. Harrison [34]. They reported the results in the application of Shape Memory Polymer (SMP) technology to the Active Disassembly of modern mobile systems. With the fasteners made of these smart materials, it is possible for products to disassemble themselves at specific triggering temperatures in an oven-like disassembly line. They applied this smart material technology to various types of mobile phones and achieved cost effectiveness and apparent time performance.

An efficient, environmentally friendly system for CRT disassembly and cleaning was designed and demonstrated by E. S. Geskin, B. Goldenberg and R Caudill [35]. They adopted waterjet technologies capable of effectively and efficiently cutting CRT's in order to separate the faceplate from the funnel. The developed technology is capable of separating CRT's at the frit line or just below in order to achieve both high-lead cullet output compositions. This capability extended potential secondary markets for recovered CRT glass to include architectural and construction applications by avoiding the environmental concern for lead glass.

In contrast to the literatures mentioned above, D. Studny et al [36] proposed to apply the destructive disassembly procedure based on impact mechanics, and provided rigorous investigation on the mechanical aspect of the disassembly process. In their research, they applied lateral impact on the head of joining element to cause shear fracture on neck area. They adopted 'instrumented bar' (Kolsky, [37]) between the striker and screw head in order to measure and apply impact load (see Figure 2.2). By comparing the pulses before and after the reflection at the screw head, they evaluated the energy invested in fracturing the screw head. Having this 'instrumented bar' in between the screw and the striker is advantageous in practical design application since it ensures a predictable contact surface to transmit stress waves and to position where the impact is applied.

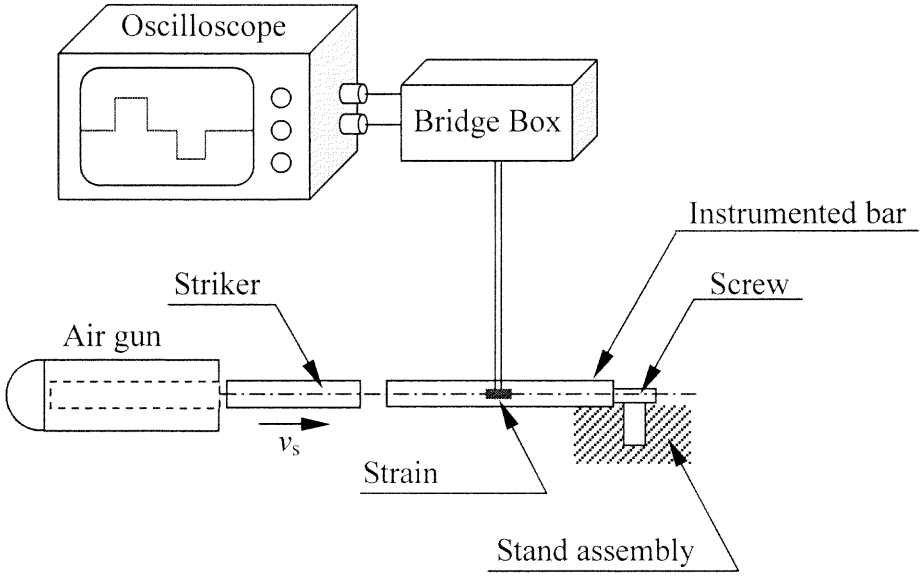

Figure 2.2 Side impact for destructive disassembly.

The striker launched by an air gun hits one end of the instrumented bar and generates a stress wave. This stress wave travels toward the other end where the

instrumented bar and the screw head are contacting each other. At the contacting surface, the stress wave reflects after losing some of its energy transmitted to the screw and stand assembly and travels back toward the struck end. The energy transmitted to the screw head causes fracture in the neck area of the screw if it generates higher stress than the dynamic strength of the bolt neck. The strain gauges attached in the mid-length of instrumented bar measure the stress waves before and after the reflection. Then the reflected stress wave is corrected using the dispersion corrections along with the damping factor, and is shifted forward in time to coincide with the stress before reflection. From the differences between the stress waves before and after reflection, the time histories of force and energy invested into fracture are calculated. The experiments were conducted on commercial stainless steel and carbon steel screws with diameters ranging from 2.0 to 5.0 mm, which are commonly used in standard commercial electronic systems. They provided quantitative investigation on the fracture energy of various types of screws and related them with the net fracture area and thread root radius. In their report, they showed the feasibility of using dynamic impact to fracture screwed fasteners in disassembly processes and integrated their results into the preliminary design of a robotic disassembly device. However, in spite of their rigorous study on the fracture energy and quantitative test results, it is needed to investigate more in the theoretical aspect of impact in order to improve the efficiency of the process.

CHAPTER 3

IMPACT MECHANICS IN DESTRUCTIVE DISASSEMBLY

3.1 Introduction

Application of mechanical impact on a protruded head of joining element is introduced as a robust destructive approach for optimizing disassembly processes. This approach consists of fracturing the neck area of joining element by applying side impact. Specifically, instead of applying impact directly with a moving striker to the head of joining element, a one-dimensional bar is placed in between them and transfers the impact force to the head of joining element. Studny, Rittel and Zussman [36], in their research on impact fracture of screws for disassembly, adopted this one-dimensional bar to measure stress waves with strain gauges attached on it. With the measured stress waves, they were able to calculate input forces to screw heads and fracture energy. They investigated the correlation of total fracture energy to different parameters such as: net fracture area and thread (notch) root radius, and provided fractographic analysis. However, to understand more of the impact mechanism involved in the process of transmitting the impact energy to the bolt head, more investigation is required in the theoretical aspect of impact.

In this research, contrast to the work of Studny et al. [36], the focus will be placed on the impact mechanisms before the fracture begins at the neck of joining element. The force and the stress applied to the bolt head will be formulated with the physical parameters of the striker, transmitter (instrumented bar) etc., and a new method that improves the efficiency of impact-destructive disassembly process will be suggested.

This research adopts the analysis of Timoshenko and Goodier [38] to develop

equations representing the stress waves and forces generated by the impact. The method that will be presented in this research has its basis on B. Hopkinson's experiment. In his experiments, he was able to measure the maximum tensile stress at the top of the steel wire that is suddenly stretched by a falling weight onto a clamp attached to the bottom of the wire. He showed that in certain condition the maximum tensile stress occurs when the stress wave has its second reflection at the top of the wire, instead of its first reflection [37]. When stress wave reflects at the top of the wire for the second time, the maximum stress was higher than the stress at the first reflection.

In this research, the type of impact-destructive method is categorized and defined according to the number of reflections of the stress wave at the bolt-contacting surface. If it is designed to create maximum stress when the stress wave reflects at the bolt-contacting surface second or subsequent period, it is defined as Multiple Reflection of Stress Wave (MRSW) Method. If the maximum stress occurs only at the first reflection at the bolt-contacting surface, and this should cause fracture at the bolt, it is defined as Single Reflection of Stress Wave (SRSW) Method.

3.2 SRSW Method

When the length of stress wave is short so that the front end of the wave does not overlap with its tail end in the same direction at any place along the transmitter bar, the maximum stress at the bolt neck occurs only at the first reflection of the stress wave. The experiment conducted by D. Studny [36] falls into this case. In their setup, the material and the diameter of striker are identical to those of the transmitter ('instrumented bar'), however the length of the striker is set relatively shorter than that of the transmitter. In this case, the stress wave is a rectangular-shaped pulse. Therefore, no matter how fast

the striker hits, the pulse duration ends before the front end of the reflected wave reaches back to the struck end of the transmitter. The pulse duration varies not with the speed but with the length of the striker, and the magnitude of the stress depends only on the speed of the striker. Therefore, the maximum stress occurs at the front of the wave and this should cause the fracture on the bolt neck when it first reflects at the bolt-contacting surface. In this case, the maximum stress in the transmitter is given by:

$$\sigma_0 = \frac{1}{2}\rho c_L \upsilon_s \tag{3.1}$$

where:

σ: stress in transmitter
ρ: material density of transmitter
c_L: longitudinal wave velocity in transmitter
v_s: speed of striker

If the cross section area of the striker is much larger than that of the transmitter bar as shown in Figure 3.1, and the material of both the transmitter and the striker is identical, the initial stress in the transmitter bar at the moment of impact can be written as:

$$\sigma_0 = \rho c_L \upsilon_s \cong \rho c_L \upsilon_s \frac{1}{(1 + \frac{A_t \rho_t c_t}{A_s \rho_s c_s})} \tag{3.2}$$

where:

A_t, A_s: section area of transmitter and striker respectively (in this case, $A_t << A_s$)
c_t, c_s: longitudinal wave velocity in transmitter and striker respectively
ρ_t, ρ_s: material density of transmitter and striker respectively

In this case, the profile of the stress wave has an inverse of exponential curve as $\sigma(t)$ in Figure 3.1(a). This stress wave proceeds toward the bolt-contacting end and reflects at

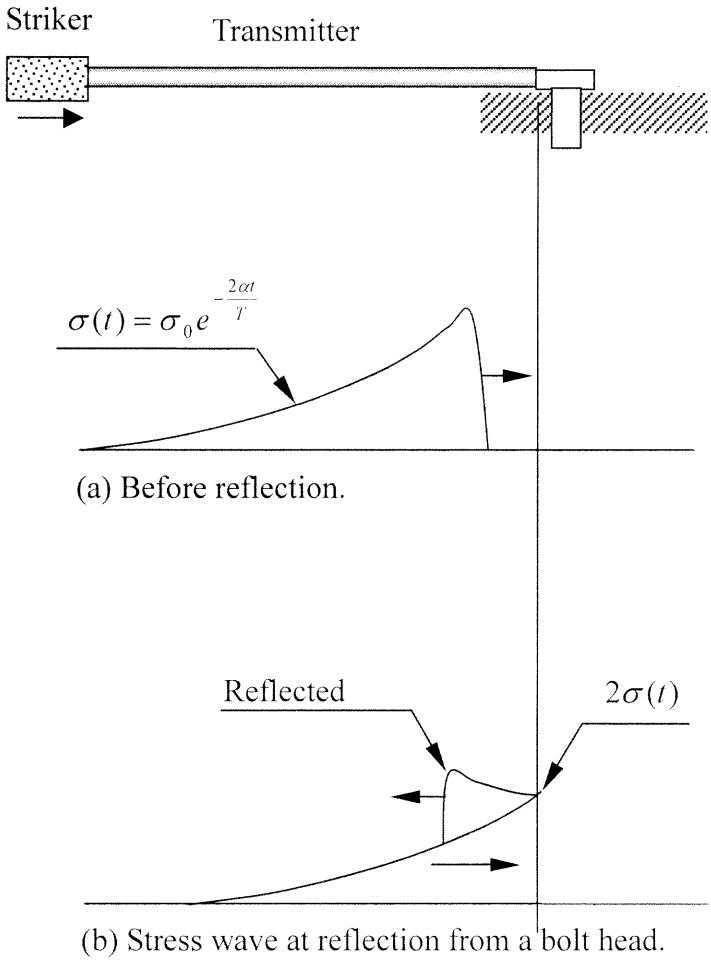

Figure 3.1 Single reflection of stress wave from a rigid bolt head.

the interfacing surface. If the bolt is mounted on a rigid body, the stress at the interface is $2\sigma(t)$ and the shear stress on the bolt neck can be written as

$$\tau_b = 2\frac{A_t}{A_b}\sigma(t) \tag{3.3}$$

where A_b is the section area of the bolt neck.

The force that will cause fracture of the bolt head can be calculated from the stress equations given above. In both cases, whether the stress wave is rectangular-shaped or an inverse of exponential form, the maximum stress occurs when the stress wave reflects at the bolt-contacting end in the first contact, and this maximum stress should be higher than the dynamic shear strength of the bolt head to cause fracture.

3.3 MRSW Method

When the length of stress wave is very long so that the front end of the stress wave overlaps with its tail end more than once in the same direction, the maximum stress at the bolt neck is higher than it occurs in single reflection. Suppose that the striker and its speed are remained as in Figure 3.1, and the transmitter bar is replaced with much shorter one. Then the time needed for the wave front makes a round trip become short, and the wave front can travel back and forth along the transmitter bar between the struck end and the bolt-contacting end until the striker stop generating compressive stress wave at the struck end (see Figure 3.2). Therefore, the compressive stress wave superpose itself twice or more than twice at the bolt-contacting end, and produce higher stress than it does with single reflection. Then the maximum stress occurs when the wave front reflects in second or subsequent period instead of occurring at the first reflection. The maximum stress in this case is higher than in the SRSW Method even if the same striker with the same speed generated the impact. In other words, higher stress can be applied to the bolt head with the same amount of energy invested on launching the striker if the mass and the length of the transmitter are reduced. However, this method requires the condition that the body on which the bolt is mounted has enough inertia so that the whole

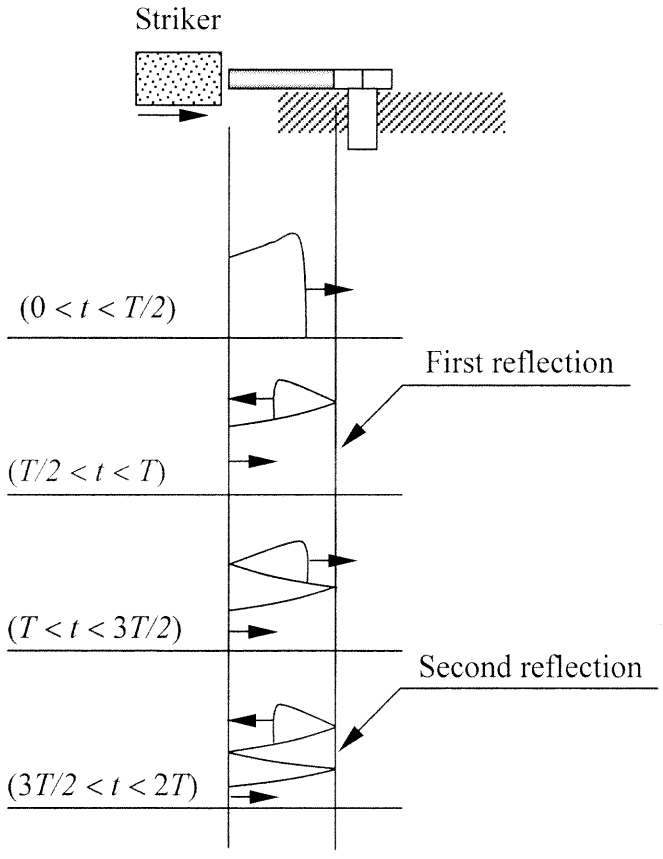

Figure 3.2 Multiple reflection of stress wave from a rigid bolt.

assembly supports the bolt, and do not move away until the maximum stress occurs. In addition, the material and structural strength of the bolt-mounted body need to be strong enough to withstand the stress transmitted from through the bolt. More precisely, the deformation of the bolt-mounted body should be remained within the elastic boundary during the whole process of impact. If it is assumed that the bolt is mounted on a rigid body, and the bolt is assumed as rigid, the problem can be solved as 'a bar with a fixed end struck by a moving mass at the other end' introduced in many literatures [37][38][39][40][41]. However, in most of practical situation, the bolt-supporting body would be non-rigid. In other words, when the stress wave reflects at the bolt-contacting

surface, some of its energy will be lost and dissipated into the bolt mounting body. Then the magnitude of the reflected wave will be reduced, and this will affect the forming of the wave equation of the subsequent period. Therefore, it is required to develop new equations for the stress wave forming after the first reflection.

3.3.1 Determination of l_t to Apply MRSW Method

Keeping the diameter of transmitter constant and using identical striker, multiple reflections can be generated at the bolt head by simply reducing the length of the transmitter. Theoretically, the length of the transmitter for MRSW Method should be determined so that the stress at the struck end has not decayed to zero when the front end of stress wave complete the first round trip. Furthermore, in order to have a noticeable effect of stress increase with MRSW Method, the stress at the struck end need to be much more than zero at that moment. In this research, it is defined that the stress $\sigma_1(t)$ at the struck end calculated from the equation (3.4) is greater than 10% of its initial stress σ_0

$$\sigma_1(t) = \sigma_0 e^{-\frac{2\alpha t}{T}} \tag{3.4}$$

when $t = 3T$. Therefore, substituting t with $3T$ in (3.4), the following condition need to be satisfied:

$$e^{-6\alpha} \geq 0.1 \tag{3.5}$$

The condition of (3.5) yields

$$\alpha \leq 0.38 \tag{3.6}$$

Therefore, the mass of transmitter needs to be smaller than 0.38 times of the mass of the striker in order to observe a noticeable effect of MRSW Method.

3.3.2 Efficiency of MRSW Method

Increase of maximum stress by reducing the mass ratio can be evaluated in comparison with the maximum stress in SRSW Method. The efficiency of MRSW Method is defined in this research as the percentage of increased amount of stress to the maximum stress in SRSW Method. This relationship can be written as:

$$Efficiency = \frac{\sigma_{max\_MRSW} - \sigma_{max\_SRSW}}{\sigma_{max\_SRSW}} \times 100(\%) \tag{3.7}$$

CHAPTER 4

EQUATIONS FOR STRESS WAVES IN A BAR CAUSED BY IMPACT

4.1 Stress Wave Equation When Bolt is Mounted on a Rigid Body

If bolt is assumed rigid and is mounted on a rigid body, the classical representation and analysis of stress waves in one-dimensional bar can be applied. In this case, the problem can be treated as that one end of the bar is fixed at an infinite rigid wall and the other end is struck by a rigid mass [38][39][40]. With one-dimensional stress wave theory, the relationship between the stress at bolt head and the parameters of the instruments including the striker and the transmitter can be formulated.

Schematic of instrument setup for applying impact on a bolt head for fracture is shown in Figure 4.1.

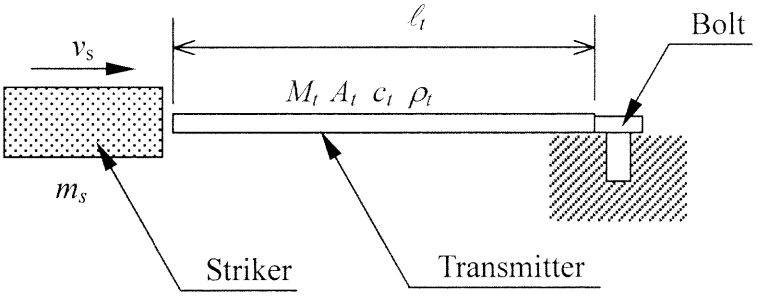

m_s: mass of striker
M_t: mass of transmitter
A_t: section area of transmitter
M_s: mass of striker per unit area of the cross section of transmitter (= m_s/A_t)
v_s: speed of striker
ρ_t: material density of transmitter
c_t: wave speed in transmitter

Figure 4.1 Schematic of instrument setup for impact fracture of bolt.

When a rigid striker of mass m_s impinges with speed v_s on one end of transmitter, the stress σ_0 at the head of the stress wave is given by the equation:

$$\sigma_0 \cong \rho_t c_t v_s \tag{4.1}$$

According to the analysis by Johnson [39] and Spott [40], the stress wave generated by the impact at the struck end of the transmitter during time $0 < t < T$ can be derived from the equation of motion for M_s as

$$M_s \frac{dv_1}{dt} = -A_t \sigma_1 \tag{4.2}$$

where σ_1 is the stress intensity at the struck end of transmitter at time t after first contact; v_1 is the particle speed of the transmitter at the struck end. Solving above equation, the stress wave in the transmitter during $0 < t < T$ is

$$\sigma_1(t) = \sigma_0 e^{-\frac{2\alpha t}{T}} \tag{4.3}$$

where $\alpha = M_t / M_s$ and $T = 2\ell_t / c_t$.

This compressive stress wave propagates from struck end toward the bolt-contacting surface at the speed of c_t, the propagation speed of the dilatational stress wave. The stress at the bolt-contacting surface is zero until $t = \ell_t/c_t = T/2$, and it suddenly becomes $2\sigma_1$ right after the front end of the wave is reflected at this surface. The stress at bolt-contacting end σ can be written as

$$\sigma(t) = 2\sigma_1 \ (t - T/2), \ \ (T/2 \le t \le 3T/2) \tag{4.4}$$

This means that the stress at the bolt-contacting end is twice the stress on the struck end during this period.

The head of the reflected wave travels back to the struck end, and generates more

stress between the striker and the transmitter from $t = 2l_t/c_t$, and again, travels toward the bolt-contacting surface. Therefore during this period, the striker faces more resistance after $t = 2\ell_t/c_t$, and since this returned wave affects the striker initiating stress, the stress wave equation for $T < t < 2T$ needs to be redefined. When the stress wave is being reflected at the struck end during this period it provides a compressive stress of $2\sigma_1$. Then the total stress $\Sigma\sigma$ at the struck end during this period would be

$$\Sigma\sigma = 2\sigma_1 (t - T) + \sigma_2(t) \tag{4.5}$$

where $\sigma_2(t)$ is the stress wave equation during $T < t < 2T$, and is to be determined. Again, the motion equation during this period can be written as

$$M_s A_t \frac{dv_2}{dt} + A_t \Sigma\sigma = 0 \tag{4.6}$$

Solving (4.6) gives

$$\sigma_2(t) = \sigma_0 e^{-\frac{2\alpha t}{T}} \left[1 + 4\alpha e^{2\alpha} \left(1 - \frac{t}{T} \right) \right] \tag{4.7}$$

This process repeats for $\sigma_3(t)$, $\sigma_4(t)$ and further, but the equations become very lengthy.

From the equations for $\sigma_1(t)$, $\sigma_2(t)$, $\sigma_3(t)$, $\sigma_4(t)$, and so on, the stresses at struck end and bolt-contacting end can be calculated. It is shown that the plots of the empirical equations solved for the fixed end give very good approximation to the theoretical curves calculated from the equations developed as above [40]. Therefore, in order for the analysis of the shear stress on the bolt neck mounted on a rigid body, the above equations can be converted to an expression for the shear stress on a bolt neck.

4.2 Stress Wave Equation When Bolt is Mounted on an Elastic Body

In most of the practical disassembly situation, the material on which the bolt is mounted cannot be treated as rigid. Thus, when stress wave is being reflected at the bolt-contacting surface some of its energy would be transmitted and dissipated into the material. Therefore, the magnitude of the stress wave after reflection becomes smaller than that of the stress wave before reflection.

Usually in a high velocity impact analysis, overall structural behavior can be ignored because deformation is concentrated at the impact point. However, in a case of a relatively low velocity of the striker or a relatively low density of the material on which the transmitter is contacting, loss of impact energy dissipated into the material need to be considered [41]. Wada [42] showed that the reflection characteristics of longitudinal wave in a semi-infinite cylindrical rod vary with the thickness of the elastic plate to which the rod is connected. He showed analytically and experimentally that when a compressive incident wave in a bar reflects at the contacting surface, the reflected stress wave gradually shifted from tensile to compressive as the plate thickness increased, which means that the rigidity of the plate affected the reflection characteristics of the stress waves. Therefore, depend on the characteristics of the material or the structure on which the bolt is mounted, the reflected stress wave at the bolt-contacting surface will have different magnitude. Figure 4.2 shows a schematic diagram of stress wave being reflected from a bolt head mounted on an elastic medium.

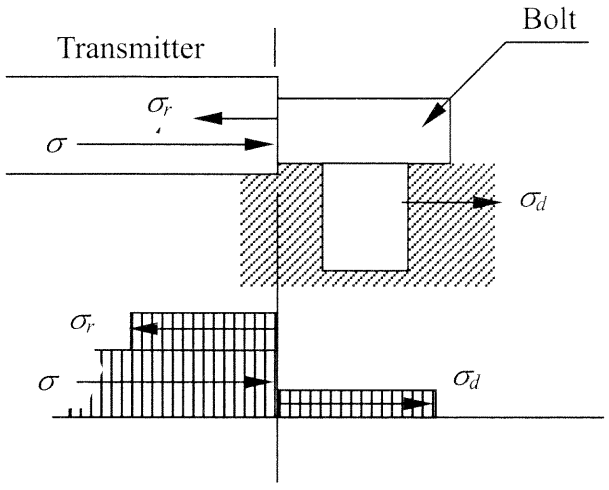

σ: stress wave before reflection
σ_r: reflected stress wave
σ_d: dissipated stress wave

Figure 4.2 Reflection and dissipation of compressive stress wave from a bolt mounted on an elastic medium.

The stress wave equation at the struck end for $0 < t < T$ is identical to (4.3) because the front of reflected stress wave has not return to the struck end in this period, therefore does not affect the equation. However, for the second period of $T < t < 2T$, the stress wave equation for this period will be different from (4.7), because the returning wave that was reflected at the bolt-contacting surface has been reduced in its magnitude. Therefore, the striker faces less resistance during this time interval than when bolt is mounted on a rigid body. Assume that there exists a ratio R ($-1 \leq R \leq 1$) between the stress before reflection and after reflection. It is reasonable to assume that the elastic wave reflects with a constant ratio R if the transmitted elastic load remains in the elastic boundary of the supporting medium or structure. Then the reflected stress wave σ_r and the transmitted stress wave σ before reflection can be related as

$$\sigma_r = R\sigma \tag{4.8}$$

When the front end of this reflected stress wave returns to the struck end of transmitter, it affects the stress wave equation for $T < t < 2T$. Then the total stress $\Sigma\sigma$ at the struck end during this period will be

$$\Sigma\sigma = 2R\sigma_I\ (t - T) + \sigma_2(t) \tag{4.9}$$

where $\sigma_2(t)$ is the stress wave equation during $T < t < 2T$ and is to be determined. The force equilibrium during this period is

$$M_s A_t \frac{dv_2}{dt} + A_t \Sigma\sigma = 0 \tag{4.10}$$

Solving the equation for second period of T, the stress $\sigma_2(t)$ is

$$\sigma_2(t) = \sigma_0 e^{-\frac{2\alpha t}{T}}\left[1 + 4R\alpha e^{2\alpha}\left(1 - \frac{t}{T}\right)\right] \tag{4.11}$$

This process repeats for the stress wave equations of $\sigma_3(t)$, $\sigma_4(t)$ and so on. Then the solutions for $\sigma_3(t)$ and $\sigma_4(t)$ can be achieved, and they are:

$$\sigma_3(t) = \sigma_0 e^{-\frac{2\alpha t}{T}}\left(A_3 t^2 + B_3 t + C_3\right) \tag{4.12}$$

$$\sigma_4(t) = \sigma_0 e^{-\frac{2\alpha t}{T}}\left(A_4 t^3 + B_4 t^2 + C_4 t + D_4\right) \tag{4.13}$$

where

$$A_3 = \frac{8\alpha^2 R^2}{T^2} e^{4\alpha}$$

$$B_3 = -\frac{4\alpha R}{T}\left\{e^{2\alpha} + R(1 + 8\alpha)e^{4\alpha}\right\}$$

$$C_3 = 8R^2\alpha(1+4\alpha)e^{4\alpha} + 4R\alpha e^{2\alpha} + 1$$

$$A_4 = -\frac{32\alpha^3 R^3}{3T^3}e^{6\alpha}$$

$$B_4 = \frac{8\alpha^2 R^2}{T^2}\left\{R(1+12\alpha)e^{6\alpha} + e^{6\alpha} + e^{4\alpha}\right\}$$

$$C_4 = -4R\alpha\left\{(12\alpha + 72\alpha^2)R^2 e^{6\alpha} + 12R\alpha e^{6\alpha} + 8R\alpha e^{4\alpha} + e^{6\alpha} + e^{4\alpha} + e^{2\alpha}\right\}$$

$$D_4 = 72(4\alpha+1)R^3\alpha^3 e^{6\alpha} + 72R^2\alpha^2 e^{6\alpha} + 4(8\alpha-1)R^2\alpha e^{4\alpha} - 8R\alpha e^{2\alpha}$$

$$+12(e^{6\alpha} + e^{4\alpha} + e^{2\alpha})R\alpha + 1$$

Overlapping the equations (4.3), (4.11), (4.12) and (4.13), the total stress at the struck end during $0 \le t \le 4T$ can be calculated for different values of R. Figure 4.3 is the plots of the normalized stress (σ/σ_0) along t/T at struck end for different values of R with α =1/4. The graph shows that the normalized stress (σ/σ_0) for R = 1.0 with α = 1/4 calculated from the developed equations is identical to the classical solutions for stress waves in one-dimensional bar fixed to a rigid wall [40]. The reason for selecting α = 1/4 is to evaluate the developed equations by comparing them with the classical solutions that provide analytical results for this particular mass ratio in rigidly fixed end case. Many different graphs can be plotted for different values of α. The stress profiles at struck end for any value of R are identical during the first period because they are not affected by the stress wave returning from the reflection. After that, the magnitude of stress gradually decreases as R decreases. Notice that the location of maximum stress shifts from $2T$ to T as R decreases from 1.0 to 0.8.

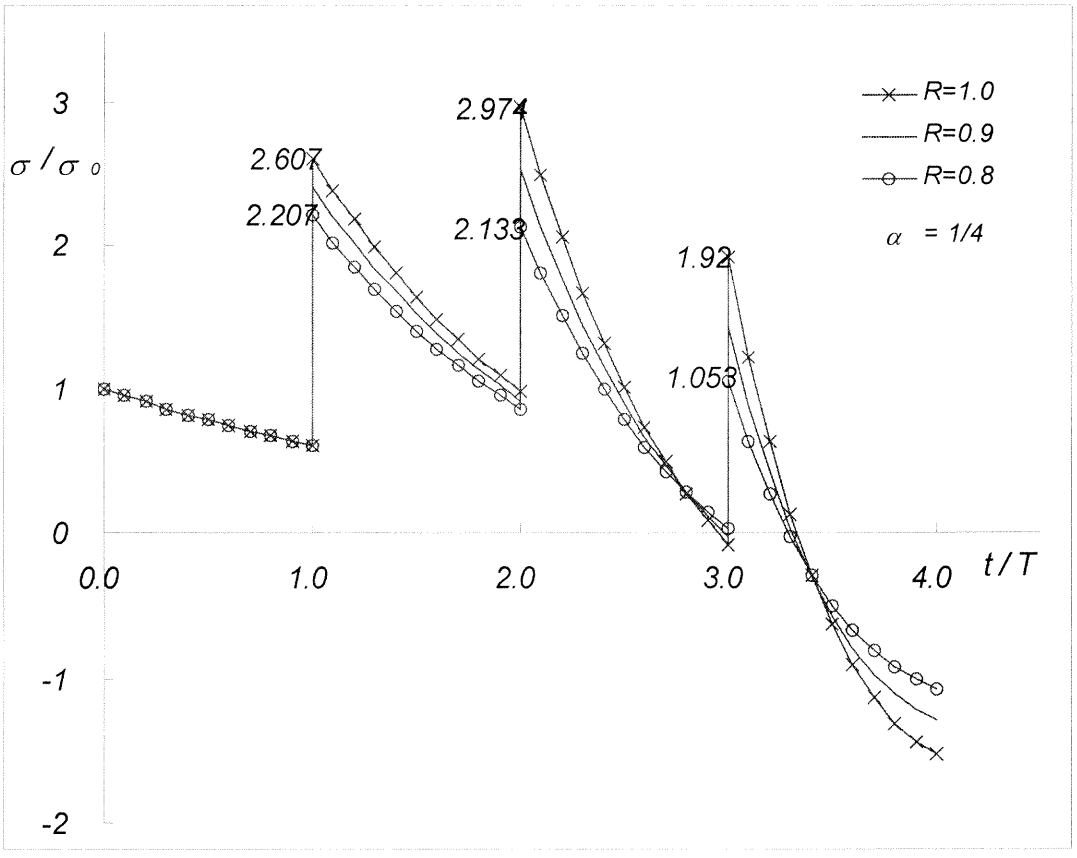

Figure 4.3 Stress ratio σ/σ_0 at struck end for different R- values.

On the other hand, the resultant stress σ at the bolt-contacting end of the transmitter is of interest since this stress can be converted as shear stress τ_b at the bolt-neck. They relate as

$$\tau_b = \frac{A_t}{A_b}\sigma \tag{4.14}$$

The shear stress τ_b should exceed the dynamic shear strength of the bolt in order to cause fracture. In the first period, the bolt head will receive no stress at all until the stress wave propagated from the struck end reaches it when $t = T/2$. Then at $t = T/2$, the resultant stress suddenly becomes $2\sigma_I(t) - \sigma_d$, and will last until $t = 3T/2$. Since $\sigma_d = \sigma_I(t) - R\sigma_I(t)$,

the resultant stress at the bolt-contacting end can be written as

$$\sigma = \sigma_1(t\text{-}T/2) + R\sigma_1(t\text{-}T/2), \quad (T/2 < t < 3T/2) \tag{4.15}$$

Similarly, the resultant stress that the bolt head is receiving from the transmitter for continuing periods can be derived, and they are

$$\sigma = \sigma_2(t\text{-}T/2) + R\sigma_2(\text{t-}T/2) + R\ \sigma_1(\text{t-}3T/2) + R^2\sigma_1(\text{t-}3T/2), (3T/2 < t < 5T/2) \tag{4.16}$$

$$\sigma = \sigma_3(t\text{-}T/2) + R\sigma_3(t\text{-}T/2) + R\ \sigma_2(t\text{-}3T/2) + R^2\sigma_2(t\text{-}3T/2)$$

$$+ R^2\sigma_1(t\text{-}5T/2) + R^3\sigma_1(t\text{-}5T/2), \quad (5T/2 < t < 7T/2) \tag{4.17}$$

For the weight ratio α = 1/4, profiles of normalized stress (σ/σ_0) for different vales of R are shown in Figure 4.4. Notice also from Figure 4.4 and Figure 4.3 that the

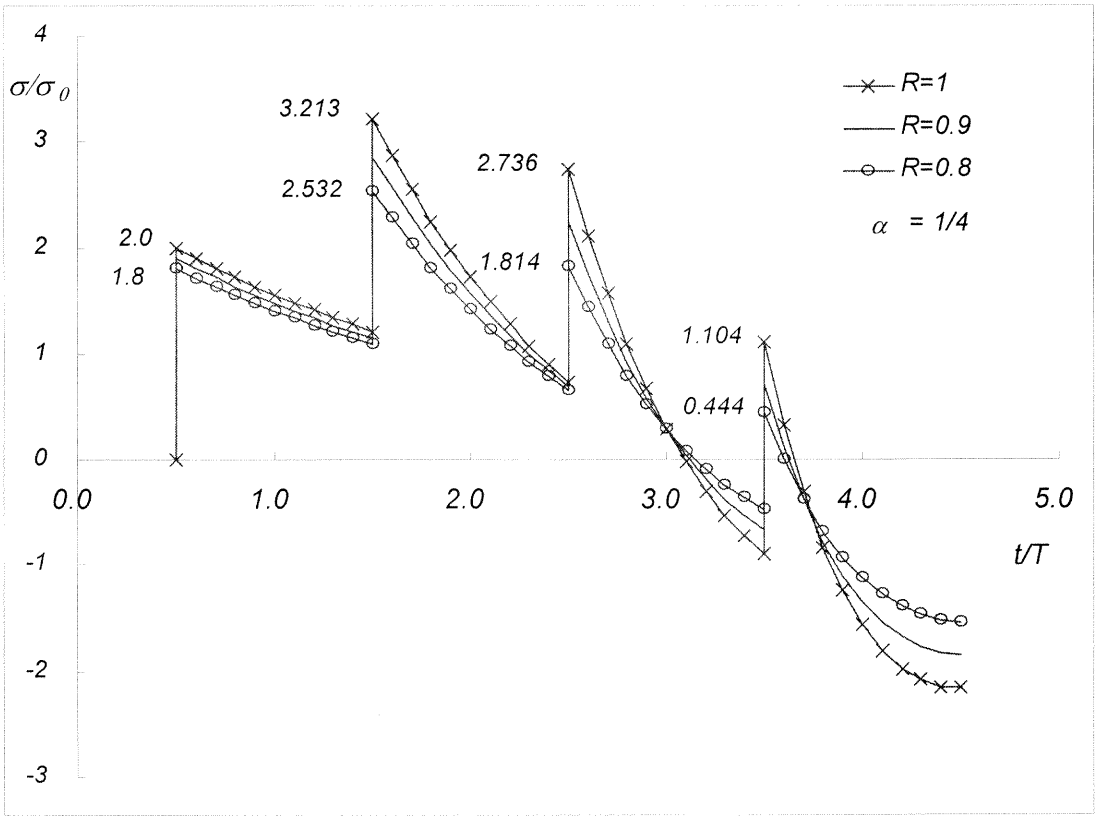

Figure 4.4 Stress at bolt-contacting end for different values of R (α = 1/4).

maximum stress at the bolt-contacting end is higher than the maximum stress at the struck end.

Using (4.14), the resultant stresses calculated from the equations (4.15), (4.16) and (4.17) can be related to the shear stress that is exerted on the bolt neck. This calculated shear stress is compared with the dynamic strength of bolt neck to analyze fracture of bolt head.

Using equations (4.15), (4.16) and (4.17), the normalized maximum stress (σ/σ_0) can be plotted for different values of mass ratio, α. The dashed curve in Figure 4.5 is a plot of the empirical equation for rigidly fixed-end case [40] that gives very good approximation to theoretical solution for R = 1.0. The curves from equations (4.15),

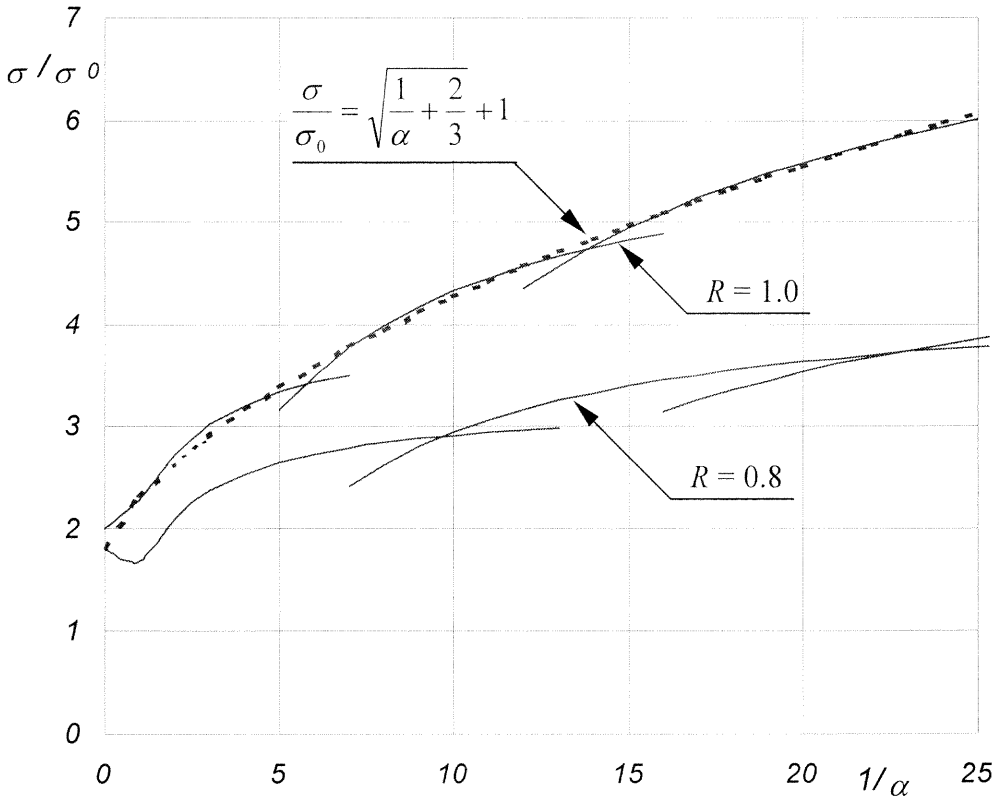

Figure 4.5 Maximum stress at bolt-contacting end for different values of mass ratio.

(4.16) and (4.17) with $R = 0.8$ are shown also for only the portion of each curve that rises above the adjoining curves. As noticed in the Figure 4.5, the maximum stress decreases significantly as the reflection ratio R decreases. This means that the effect of stress increase by adjusting mass ratio reduces if bolt is mounted on a less-rigid body.

4.3 Determining the Reflection Ratio *R*

There are limited numbers of literatures that address the reflection characteristics of stress waves in one-dimensional bar contacting with other medium. One of the researches most relevant to this issue is the one presented by Hiroshi Wada [42]. He reported the theoretical equations and the experimental results about the reflection characteristics of longitudinal elastic waves in a cylindrical rod connected perpendicularly to an elastic infinite plate. In his analysis, the motion equation of the rod in z-axis is related to the motion equation of the plate in the direction perpendicular to its surface, and the relationship between the incident wave and the reflected wave was obtained. In his experiment, strain gauges are cemented in the mid-length of the bar and one end of this bar is in contact perpendicularly with an infinite plate. The stress waves are measured before and after the reflection, and it is shown that the magnitude of the reflected wave becomes smaller as the thinner plate is being used. This implies that the ratio between the magnitude of the stress waves before and after the reflection varies with the rigidity of the plate.

However, determining the analytic value of R would be a very challenging research subject even with the bolt mounted on an ideally shaped geometry, such as, an infinite plate or an infinite half space. Unlike Wada's situation, the analysis for finding R would be very difficult because the elastic medium on which the bolt is mounted is

receiving stress in transversal direction; there exist combination of dilatation wave and distortion wave. Because the bolt is protruded, the elastic medium will also receive moment that will cause motion perpendicular to its plane. Therefore, the stress wave equation of one-dimensional bar should relate to three independent equations of motion of the elastic medium in order to find the analytic solution for R. It is even more complicated if the bolt is mounted on an arbitrarily shaped medium. With all the effort, even if an analytic solution for R were achieved for ideally shaped geometries, its implementation to practical situations would be limited. Since the reflection of stress waves is highly sensitive to material and structural characteristics of the immediate vicinity of the bolt, there will be some differences between the R-values even if they are measured from the same bolt from different directions. Therefore, for practical applications, it is desirable to investigate many different types of combination of materials and structural conditions, and broaden the knowledge about the reflection characteristics.

In this research, the reflection ratio will be determined by investigating the reflection characteristics of stress waves from a bolt head obtained from experiment. A transmitter bar with strain gauges attached in the mid-length of it will be in contact with a bolt head. The length of the transmitter bar needs to be long enough in order to separate reflected and incident waves. By generating a square-shaped incident pulse with a relatively smaller striker, the profiles of stress wave before and after the reflection from a bolt head will be measured. Then the value of R will be determined by analyzing these recorded profiles of stress waves.

4.4 Increase in Maximum Stress by MRSW Method

From the analysis of stress waves in a bar, it is possible to calculate the stress wave profiles at bolt-contacting end when each SRSW Method and MRSW Method is applied. The maximum stress at bolt-contacting end in MRSW Method is calculated much higher than in SRSW Method even when a striker hits transmitter with the same speed in both methods. In other words, the maximum stress is increased with MRSW Method even with the same amount of energy invested in launching the striker. Therefore, the efficiency of disassembly process can be improved with MRSW Method.

Table 4.1 Increase in Maximum Stress for Different Reflection Values (For $\alpha = 0.25$)

R	Maximum Stress (σ/σ_0)		Increase (%)
	SRSW Method	MRSW Method	
1.0	2.0	3.213	60.7
0.9	1.9	2.862	50.6
0.8	1.8	2.532	40.7
0.7	1.7	2.221	30.6
0.6	1.6	1.930	20.6
0.5	1.5	1.660	10.7
:			

The analysis shows that the difference in maximum stress between both methods varies depend on the reflection ratio R. If more of the stress wave energy is dissipated into the bolt-mounted medium, less the stress is increased at the bolt-contacting end in MRSW Method. For $\alpha = 0.25$, the maximum stresses in SRSW Method and MRSW

Method are calculated for different values of R and are shown in Table 4.1 with the percentile of increase.

Similarly, tables can be made for different values of mass ratio α. As indicated in the table, for $\alpha = 0.25$, the maximum stress can be increased theoretically up to 60.7% using MRSW Method if bolt is mounted on a rigid body.

CHAPTER 5

EXPERIMENTAL INVESTIGATION

5.1 Experimental Setup

Experimental setup has been prepared to evaluate the feasibility of MRSW Method. Since one of the main purposes of the experiment is to demonstrate the effect of stress increase in MRSW Method, more focus is placed on monitoring the stress wave in transmitter bar near bolt-contacting end without fracturing the bolt. The experimental process is divided into two stages. One is to acquire the reflection characteristics of the stress wave so that the reflection ratio R can be determined for further calculation of the stress wave profile near the bolt-contacting end. The other is to measure the stress wave profile near the bolt-contacting end when each SRSW Method and MRSW Method is applied. Photographic images of the experimental setup and equipments are shown in Appendix.

5.1.1 Setup for Measuring the Reflection Characteristics of Stress Wave

The experimental arrangement for the acquisition of reflected stress wave is shown schematically in Figure 5.1. A steel rod (transmitter) of 9.525 mm in diameter and 900mm in length is placed horizontally on V-shaped rubber supports. One end of the transmitter is in contact with one of six sides of the bolt head that is joining two identical steel angled beams. See Figure 5.2 for detailed configuration of the angled beam assembly. The size of the bolt and the angled beam are given in Table 5.1. When the equations are formulated, it is assumed that the contact between transmitter and bolt head is made over the entire end surface of the transmitter, and that they remain in contact for

the duration of the impact. However, these conditions are difficult to realize not only in the experiment but also in the actual disassembly processes. The length of the angled beam assembly is determined so that the time needed for the transmitted stress wave

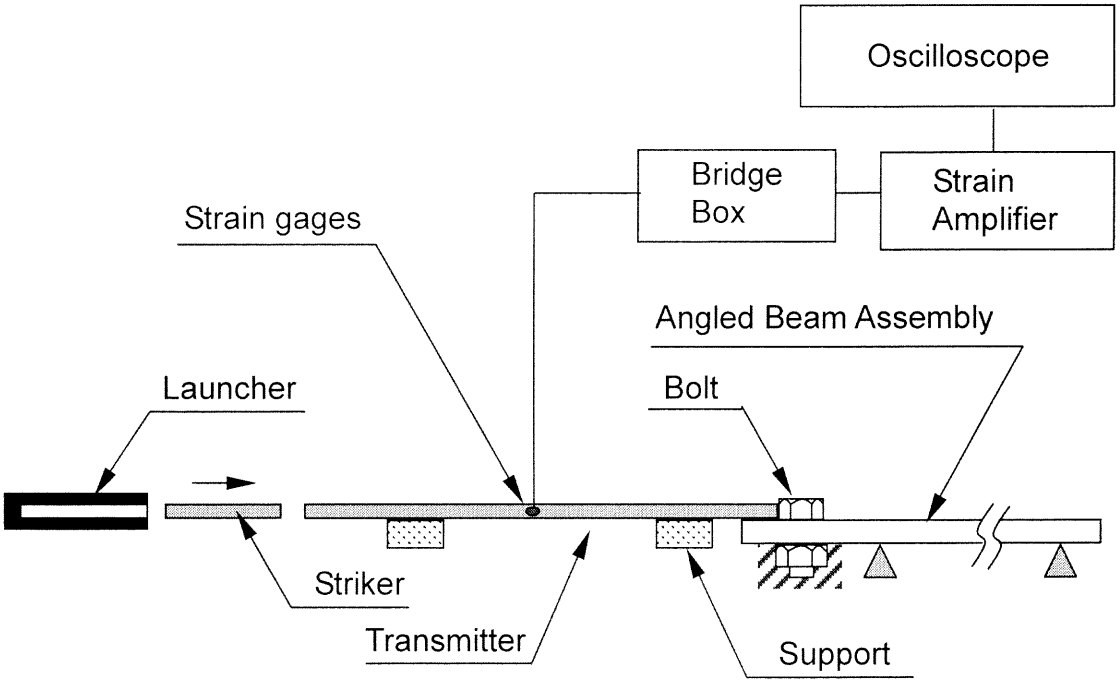

Figure 5.1 Setup for measuring reflection of stress waves.

makes a round trip from bolt head to the edge at far end is long enough. Thus, the tensile wave returning from far end of the assembly would not affect the stress wave reflections at the bolt head. The assembly of angled beams is clamped at its mid-length into a wood plate. In the mid-length of the transmitter, in order to increase sensitivity and accuracy in observing the stress waves two identical strain gauges of 3mm in length are cemented to opposite sides of the rod and connected to a bridge box. The output from the strain gauges is fed through a bridge box and a strain amplifier (VISHAY ELLIS-20) to a digital storage oscilloscope (Tektronix 2230) and the oscilloscope traces

are down loaded to a pen-plotter (HP-7470A) to produce hard copies. The internal trigger (fast-rise) in the oscilloscope is used to initiate storing the time histories of the stress waves.

The striker, launched by a spring-loaded launcher, is made of a steel rod of 270mm in length and of the same size in diameter of the transmitter. This striker hits the transmitter and generates a compressive pulse. For the length of this striker, the pulse duration is 105μs. This rectangular-shaped pulse travels toward the interface between the bolt and the transmitter, and comes back after being reflected at the interface. While this pulse travels fore- and backward, it passes the strain gauges attached in the mid-length of the transmitter, and its intensity is recorded.

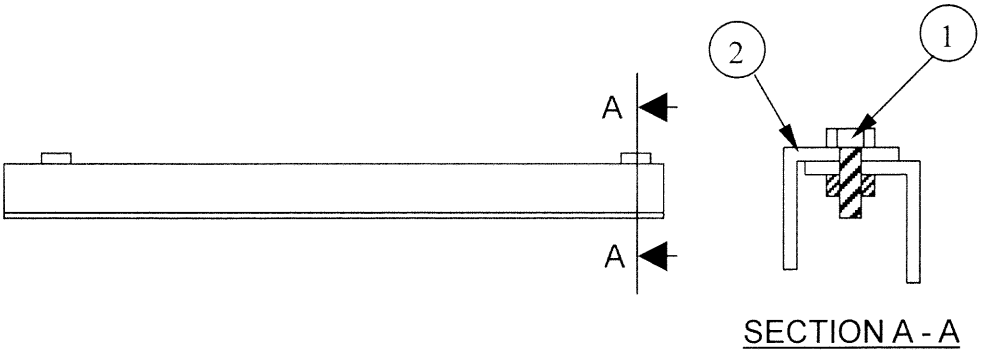

Figure 5.2 Angled beam assembly.

Table 5.1 Sizes of Bolt and Beams in the Assembly

No.	Name	Size	Material
1	Bolt	10mm-1.0 × 20mm	Steel
2	Angled Beam	50.8 × 50.8 × 915mm, t = 3.18	Steel

5.1.2 Setup for Measuring Stress Wave Profile

As shown in Figure 5.3, the incident pulses are generated by the impact of a steel block ($25.4 \times 25.4 \times 50.8mm^3$, 0.415kg) that is hung by a pendulum. The steel block, which is the striker, is attached to a pendulum of 810mm in radius with a rubber insulator inserted between them. In order for the striker to be treated as 'rigid', the striker in this setup has

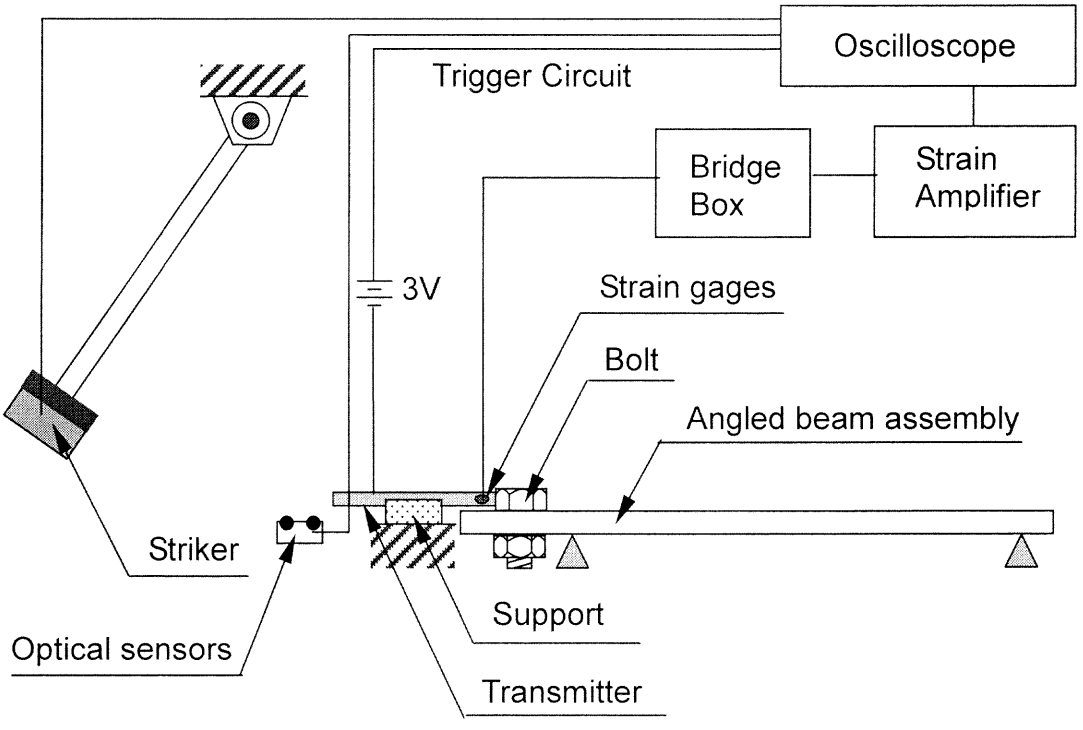

Figure 5.3 Experimental setup for measuring stress wave profile.

much larger section area than that of the striker used for investigating reflection characteristics of the stress waves. Therefore, the stress wave generated by this striker has a form of an inverted exponential curve decaying to zero over time instead of having a rectangular pulse as in the previous section.

Two different transmitters are prepared to acquire the stress wave profiles near

bolt-contacting end for SRSW Method and MRSW Method. The transmitters have the same size of diameter (9.525mm), but one has 900mm while the other has 103mm in length. Therefore, it takes 349μs for a stress wave makes a round trip in the long transmitter bar while it takes 40μs in the short one (from equation $T = 2l_t/c_t$, $T = 349\mu$s in SRSW and $T = 40\mu$s in MRSW Method). The length of the transmitter bar for the experiment of MRSW Method is determined in a way that the stress wave reflects at least three times at the bolt head. Since the striker in this experiment generates the stress wave lasting more than 200 μs until it decays to 10% of its initial stress, the stress wave in the transmitter of 103mm in length can make more than three reflections at the bolt head. The mass ratios ($a = M_t / M_s$) are 1.96 for long transmitter bar and 0.224 for short transmitter bar. Each transmitter is placed horizontally on V-shaped rubber supports. One end of each transmitter is in contact with one of six sides of the bolt head that is mounted on the angled beam assembly described in the previous section. Each of the transmitters has strain gauges cemented to opposite side of the rod approximately 14mm away from the bolt-contacting end. The strain gauges cemented on each transmitter are connected through a bridge box and a strain amplifier to an oscilloscope for monitoring stress waves. The striker of steel block hits one end of each transmitter with a same speed in order to make energy input identical for both SRSW and MRSW Methods. The stress profiles near the bolt-contacting end of each transmitter are monitored through the oscilloscope.

5.2 Reflection Characteristics of Stress Waves

5.2.1 Experimental Results

Using the experimental setup described in 5.1.1, a graph (Figure 5.4) showing the incident wave and reflected wave is achieved. Unlike the experimental results presented by Boucher [43] and Wada [42], the reflected stress wave from a protruded bolt mounted on an elastic material showed a unique characteristic. When stress wave in one-dimensional bar reflects from an infinite plate or an infinite half space, the stress wave maintained its shape although its magnitude varied according to the thickness and material properties of the plate. However, the reflected stress wave from a bolt head showed an 'unstable period' in the beginning and then gradually stabilized. It seems

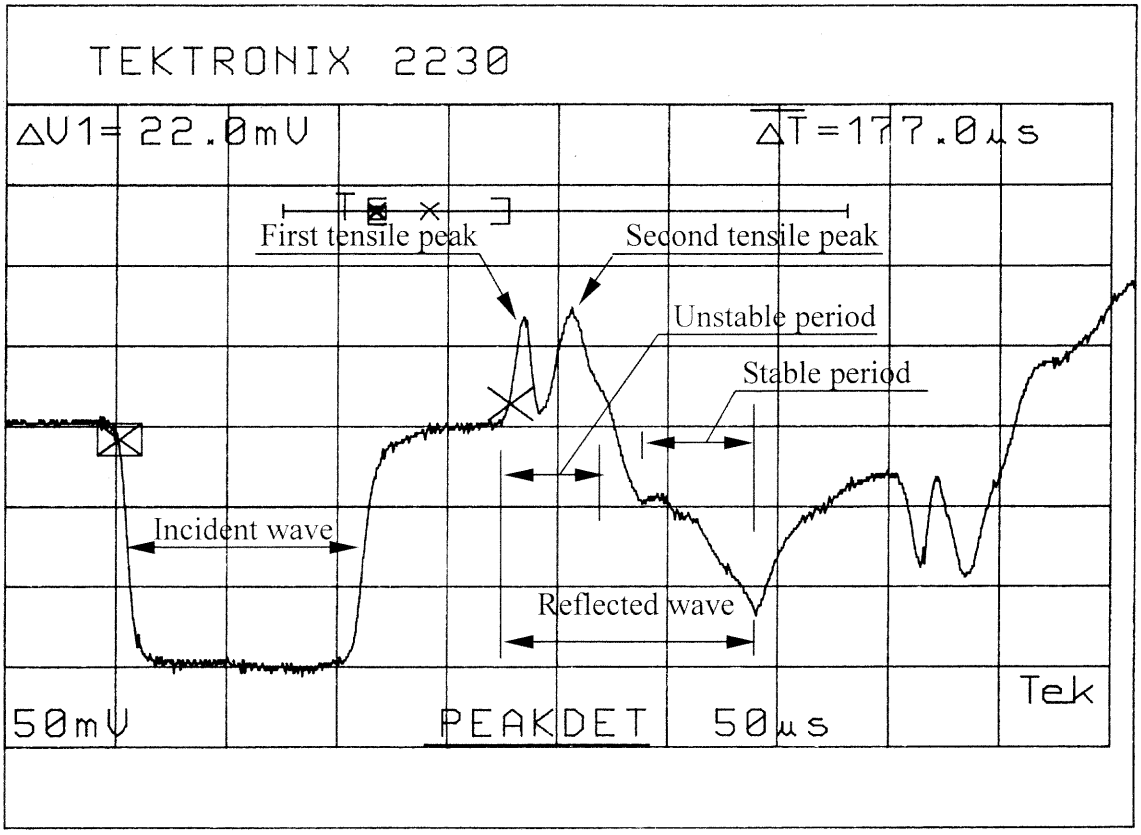

Figure 5.4 Reflection of stress wave from a bolt head.

that the 'unstable period' in the beginning of the reflected wave exists because of imperfect surface-to-surface contact between the transmitter and bolt head and also the tensile wave reflected from the other faces of the bolt head.

As shown in Figure 5.4, there are two tensile peaks in the beginning of the reflected wave. The magnitude and its duration of the first peak are depending on the contact condition between the bolt and the transmitter. If the contacting surface gets larger, the magnitude and the duration of the first peak get smaller and shorter respectively. It seems that the second tensile peak is a result of reflected wave returning from the other faces of the bolt head. In order to verify it, an experiment was conducted by placing the transmitter contacting with one edge of the angled beam assembly in the same direction as for contacting the bolt head (see Figure 5.5).

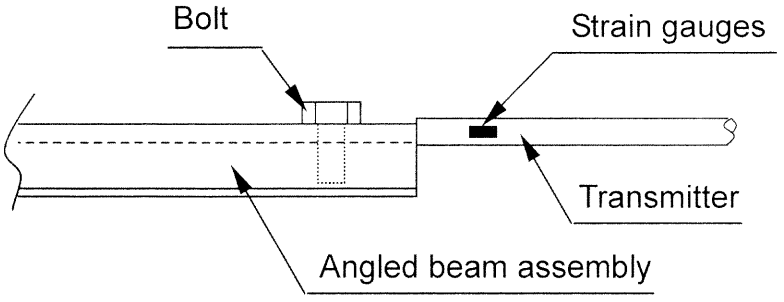

Figure 5.5 Transmitter is in contact with an edge of the angled beam assembly.

Figure 5.6 is the result and it shows the incident wave and its reflected wave from the edge of the angled beam assembly. As noticed, there exists only one tensile peak at the beginning of the reflected wave and this peak is the result of imperfect contact condition as described above. Therefore, the second tensile peak is a unique characteristic found in the wave reflection from a bolt head.

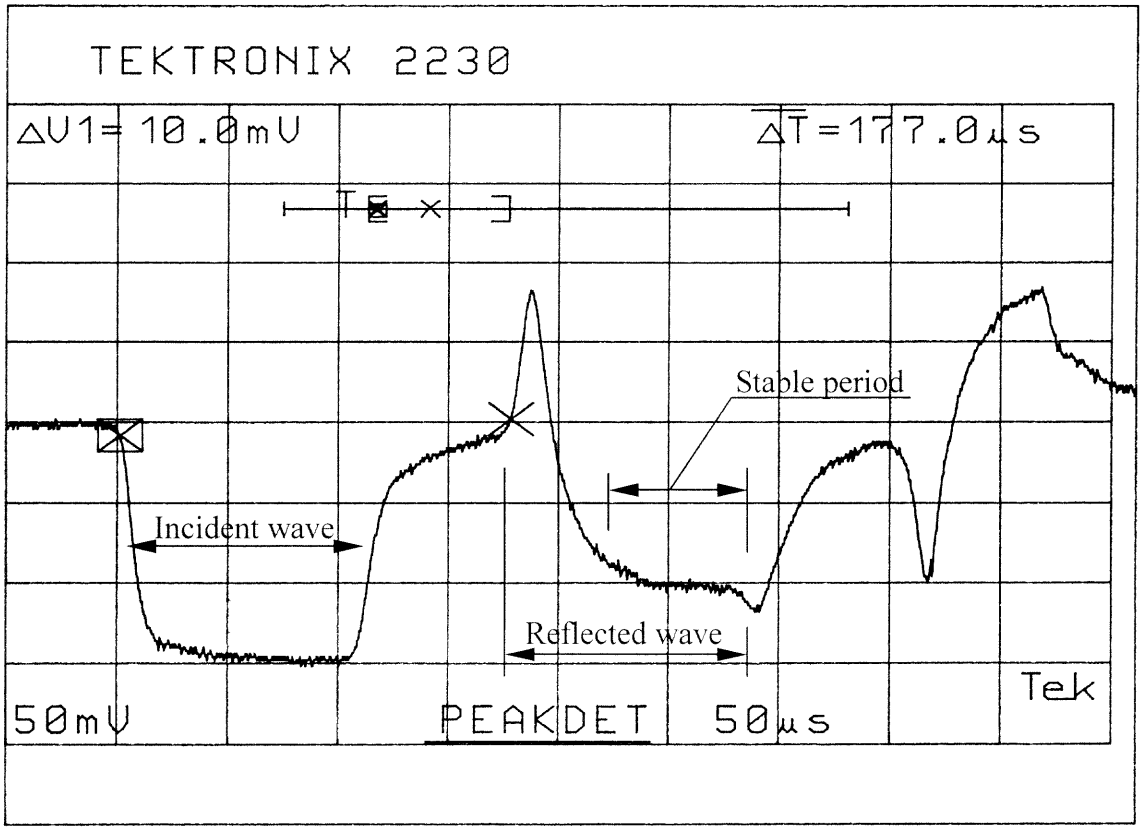

Figure 5.6 Reflection of stress wave from an edge of the angled beam assembly.

Another characteristic found in the reflected wave from a bolt head is in the 'stable period'. The magnitude of reflected wave reached rapidly to a certain level and remained constantly when the stress wave reflects from an edge of the angled beam assembly. However, the stress wave in the 'stable period' of reflected wave from a bolt head does not reach to a constant level rapidly. Its magnitude slowly increased until the tail end of incident wave reflects and escapes from the contacting surface. It is not known from this experimental setup whether the magnitude reaches to a certain level and remains constantly because the lengths of the transmitter and the striker are not long enough to measure longer time history. However, it is obvious from Figure 5.7 that the magnitude did not reach to a constant level during the first 150μs, which is enough time

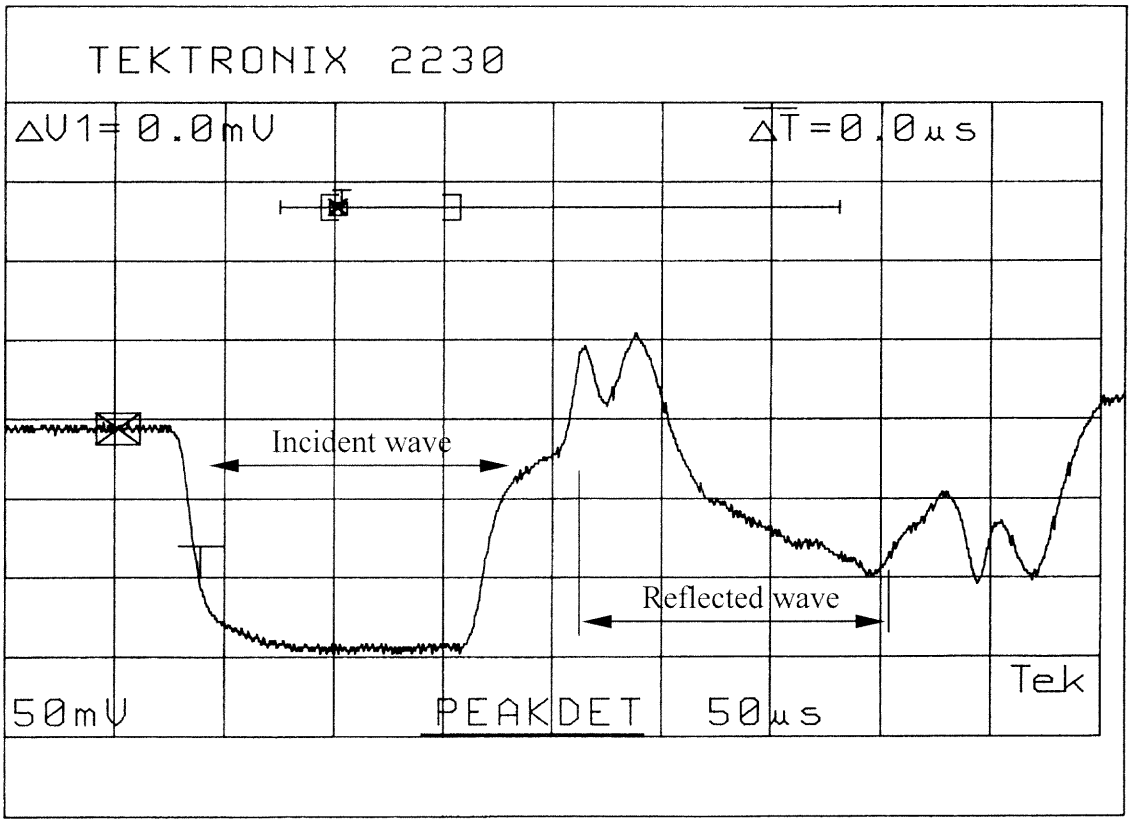

Figure 5.7 Reflection of stress wave from a bolt head (striker length = 338mm).

to monitor the stress wave when MRSW Method is applied. Figure 5.7 is the result of experiment with a striker of 338mm in length, which is almost the maximum length that can be used for the transmitter in this experimental setup.

5.2.2 Determining Reflection Ratio *R*

Those unique characteristics found in the reflected wave from a bolt head make it difficult to determine the reflection ratio. For the stress wave reflected from an edge of the angled beam assembly, the reflection ratio can be obtained simply by dividing the magnitude of the reflected wave in 'stable period' with the magnitude of incident wave. In this case, the results of stress wave analysis for both MRSW and SRSW Method would be similar to its experimental results. However, due to the tensile peaks in the beginning

and inconsistent magnitude of the 'stable period' in the reflected wave from a bolt head, the accuracy in analyzing stress waves in both methods would be affected significantly.

In order to find a closest stress wave profile, the reflection ratio is determined by dividing the average magnitude of 'stabilized period' with the average magnitude of incident wave. Since there is only one equation describing the stress profile at the bolt-contacting end for SRSW Method, the analytic stress profile during the 'stable period' obtained by applying this reflection ratio is close to the experimental result. However, the analytic stress profiles in MRSW Method obtained by using this reflection ratio are not quite accurate as much as in SRSW Method due to the 'unstable period' in the beginning of the reflected wave. It is because of the nature of how the equations are derived. Since the initial conditions for the second and further period correlate to the previous period, the 'unstable period' in the beginning will affect whole equations. Therefore, decreased stress during this 'unstable period' in the beginning will cause delay in stress accumulation in consecutive periods. This unexpected characteristic of reflected stress wave would affect the accuracy of the analysis.

For the purpose to evaluate feasibility of MRSW Method over SRSW Method, the reflection ratio determined by dividing the average values of the magnitudes is used to calculate stress wave profiles as a reference. From the experiment, the reflection ratio R is obtained as 0.52.

5.3 Numerical Analysis and Experimental Results

5.3.1 Stress Profile at the Bolt-Contacting End with SRSW Method

The physical constants for transmitter and striker are taken from the experimental setup described in 5.1.2. The optical sensors measure the speed of the striker at the moment of impact. To ensure the accuracy of experimental setup, the stress profile at struck end is measured and compared with the stress profile at struck end calculated using following equation:

$$\sigma(t) = \sigma_0 e^{-\frac{2\alpha t}{T}} \tag{5.1}$$

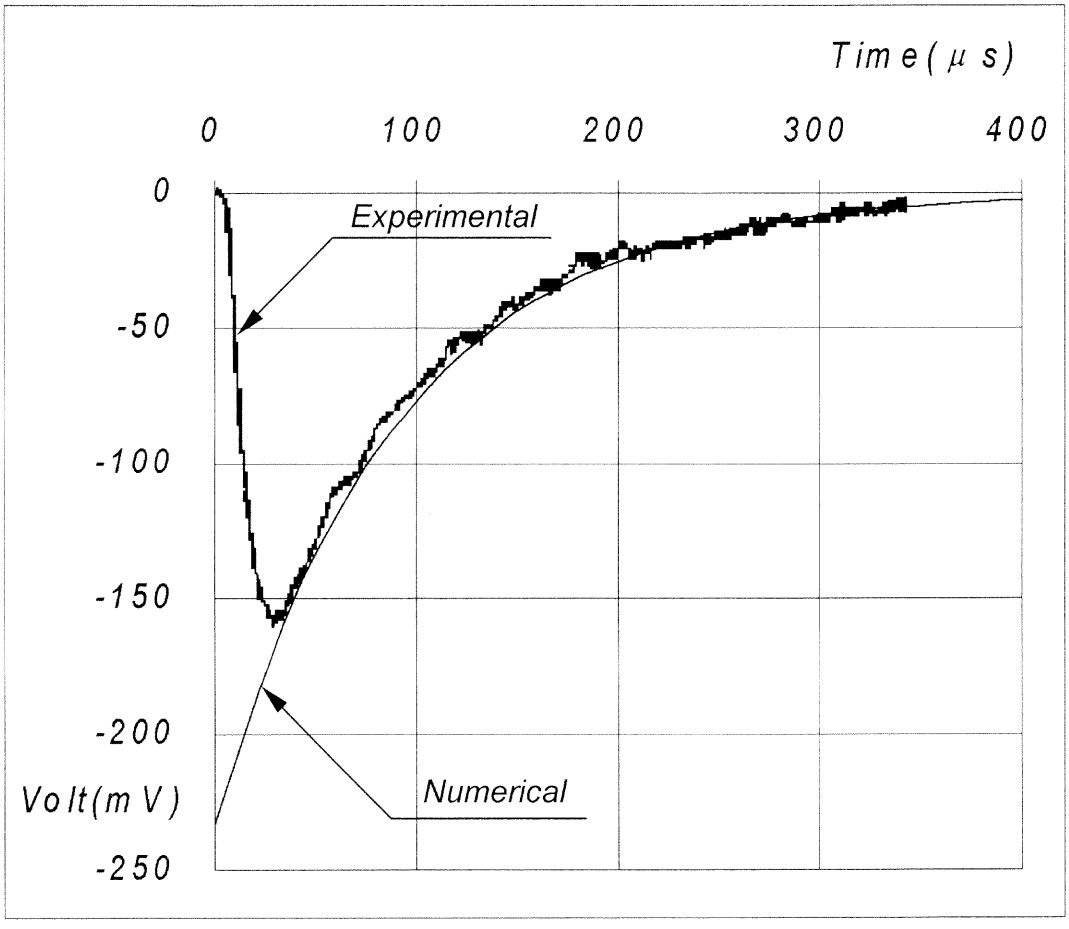

Figure 5.8 Incident pulse from equation (5.1) and its experimental result.

Until the front end of incident wave reflects and comes back to the struck end again, the measured stress wave at the struck end is purely generated by the striker. The shape of the incident wave at the struck end taken from the experiment is shown in Figure 5.8 with the graph calculated from the equation (5.1). The figure shows that the pulse shape taken from the experiment is very close to the curve calculated from the equation (5.1). This stress wave travels along the transmitter toward bolt-contacting end and reflects back toward the struck end. When this stress wave is being reflected, the stress at the bolt-contacting end can be calculated from the following equation:

$$\sigma(t) = (1 + R)\sigma_0 e^{-\frac{2\alpha t}{T}} \tag{5.2}$$

Replacing the reflection ratio R obtained from the experiment in previous section into the equation (5.2), stress profile at the bolt-contacting end is obtained as in Figure 5.9. For the time interval that matches with the 'stable period' in the reflected wave (approximately between 65μs ~140μs), the numerical curve (with R = 0.52) passes the experimental curve in the middle. It is because the reflection ratio is obtained from the averaged magnitudes of reflected wave and incident wave during this period. After 135μs, the experimental curve follows the numerical curve calculated with R = 0.9 for a while. The reflection characteristics of this time region (after around 150μs) are not known from the previous experiment examining the reflections of stress waves. As shown in Figure 5.9, the maximum stress is generated near the moment when the stress wave contacts bolt head in the beginning. Then after the 'unstable period', stress rises again and gradually decreases similarly to numerical curve. Therefore, depend on the contact condition between the transmitter and the bolt, maximum stress may occur at the first peak during 'unstable period' or when the stress rise again in 'stable period'. In this

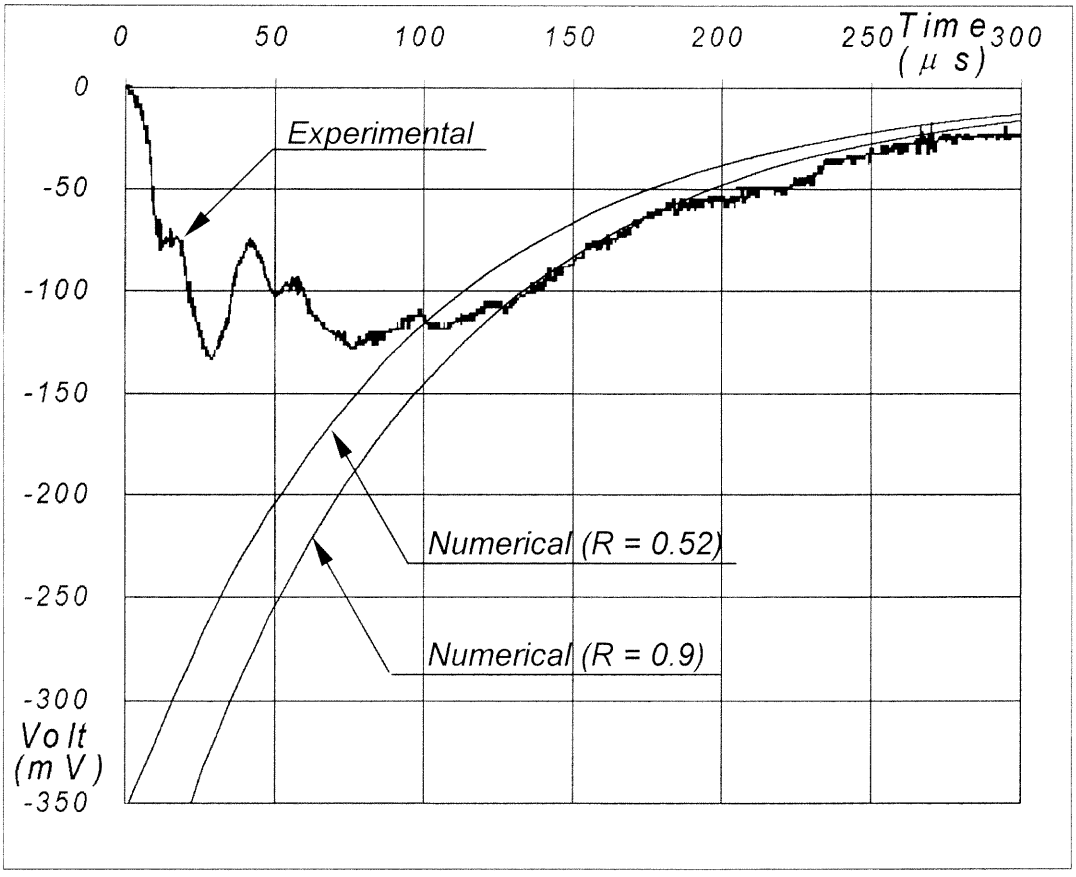

Figure 5.9 Stress at bolt-contacting end (SRSW).

experiment with SRSW Method, the maximum stress at the bolt-contacting end occurred at the first peak and is measured as σ_{max} = 144.6MN.

5.3.2 Stress Profile at the Bolt-Contacting End with MRSW Method

The length of the transmitter is shorter in this case. Therefore, the mass ratio α and the time required for the stress wave make the first round trip T are different from the ones used for SRSW Method in the previous section. The numerical stress wave profile at the bolt-contacting end is obtained by substituting the parameters in the equations developed for MRSW Method and shown with its experimental result as in Figure 5.10. Since the strain gauges are attached approximately 90mm away from the struck end, it

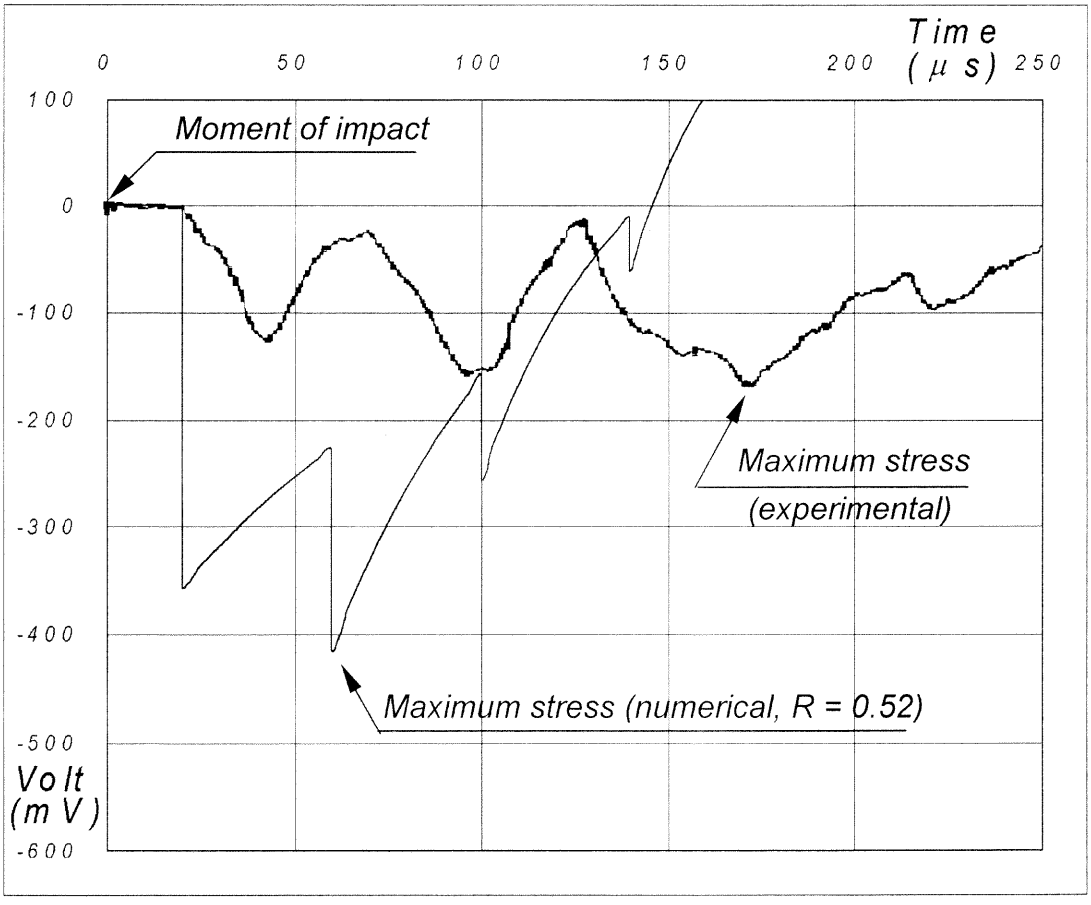

Figure 5.10 Stress at bolt-contacting end (MRSW).

takes about 18μs for the stress wave to reach them. The numerical curve shows the maximum stress occurs at the second peak. However in the experiment, due to the stress decrease during the 'unstable period', the stress did not rise as much as expected at the beginning of the reflection. The stress at the first peak is 142.4MN, and that is almost the same magnitude of maximum stress measured in SRSW Method. Then the stress continues to rise in the consecutive peaks, and the maximum stress is generated at the third peak. In this experiment with MRSW Method, the maximum stress at the bolt-contacting end is measured as σ_{max} = 183.44MN.

5.3.3 Increase in Maximum Stress by MRSW Method

As noticed in the experiments, the tensile peaks in the beginning of reflected stress wave from a bolt head caused decrease in maximum stress significantly for both SRSW and MRSW Methods. Since the analysis shows that the stress wave in SRSW Method has its maximum stress in the front end, these tensile peaks in the beginning of reflection affected directly reducing the maximum stress. For the stress waves in MRSW Method, the reduced stress due to the tensile peaks in the beginning of reflection caused the initial condition of stress wave in the second period reduced, and consequently, affects subsequent periods. Therefore, the maximum stress in MRSW is also reduced due to the tensile peaks in the beginning of the reflected stress wave. However, even with this

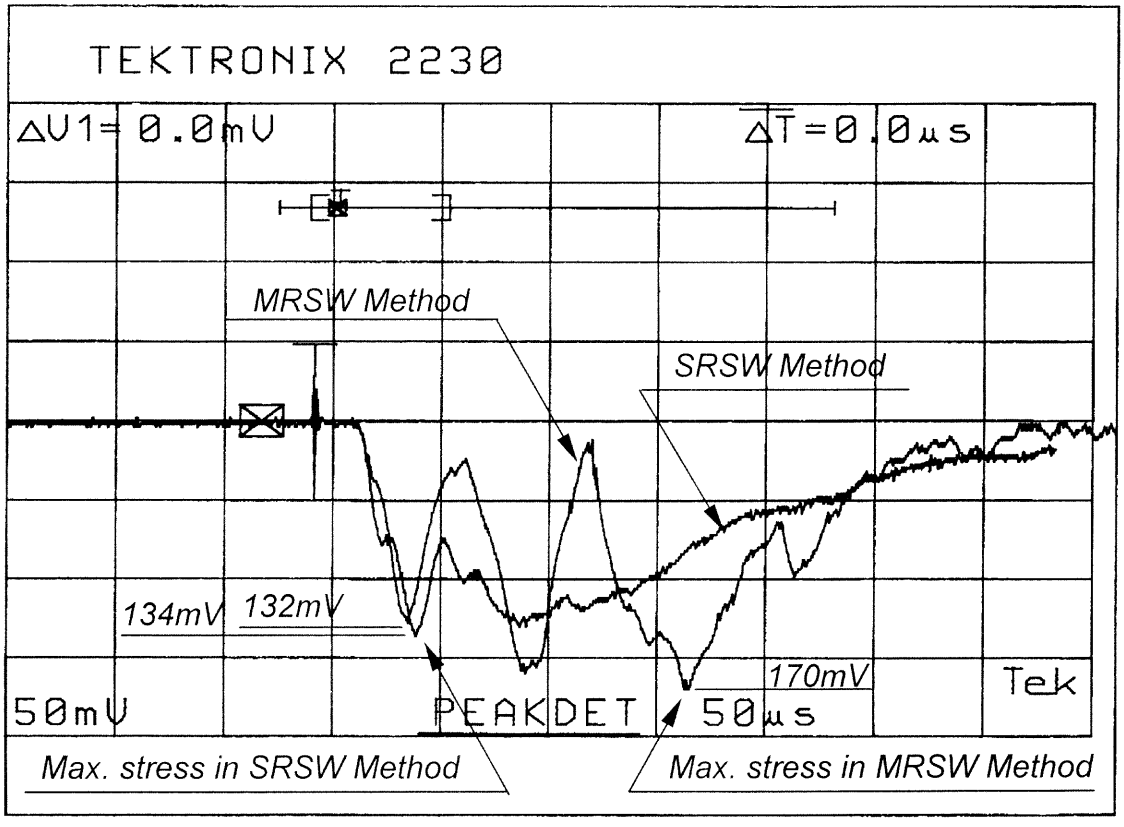

Figure 5.11 Stress profiles near bolt contacting end (Experimental result).

unfavorable reflection characteristic, the maximum stress was increased in MRSW Method compare to SRSW Method as the stress wave accumulated in the 'stable period'. In Figure 5.11, the time histories of stress waves measured near the bolt-contacting end in both methods are shown overlapped together.

The stress wave profiles in both methods showed similarity during the 'unstable period'. However, as they go into the 'stable period' the maximum stress in MRSW Method has increased while the stress in SRSW Method gradually decreased. As shown in Figure 5.11, the maximum stress is placed in the beginning of the impact in SRSW Method while the maximum stress is placed around 150μs after the beginning of the impact in MRSW Method. In this experiment, the maximum stress is increased 26% in MRSW Method using the same striker with the same speed used in SRSW Method.

5.4 Applying Impact on a Smaller Bolt Head

A set of experiments is conducted to investigate how the size of a bolt head affect the reflection characteristics and stress profiles in both SRSW Method and MRSW Method. Since the size of bolt head is smaller than the one used in the previous experiments, the contact surface between the bolt head and the transmitter is significantly reduced. In the analysis of reflection and transmission of compressive stress waves between bars, the contact surface area between bars is an important parameter. Therefore, smaller bolt size would affect the reflection characteristics and the stress wave profiles of SRSW and MRSW Methods.

The experiments presented in this section will show how smaller size of a bolt affect the reflection characteristics and the efficiency of increasing maximum stress using MRSW Method.

5.4.1 Experimental Setup

The experimental setup is identical to the one used in the previous section, except the smaller bolt mounted on the other end of the angled beam assembly. The size of the bolt is 0.8mm-1.5 × 25mm, and is made of steel. Since the size of the contacting surface area between the bolt head and the transmitter is of interest, one of six side-faces of the bolt head is measured, and compared with the contacting surface area of the larger bolt head. As shown in Figure 5.12, the size of contacting surface area between the transmitter and the smaller bolt head (View B) is half the size of the contacting surface area with a larger bolt head (View A) in the previous experiments.

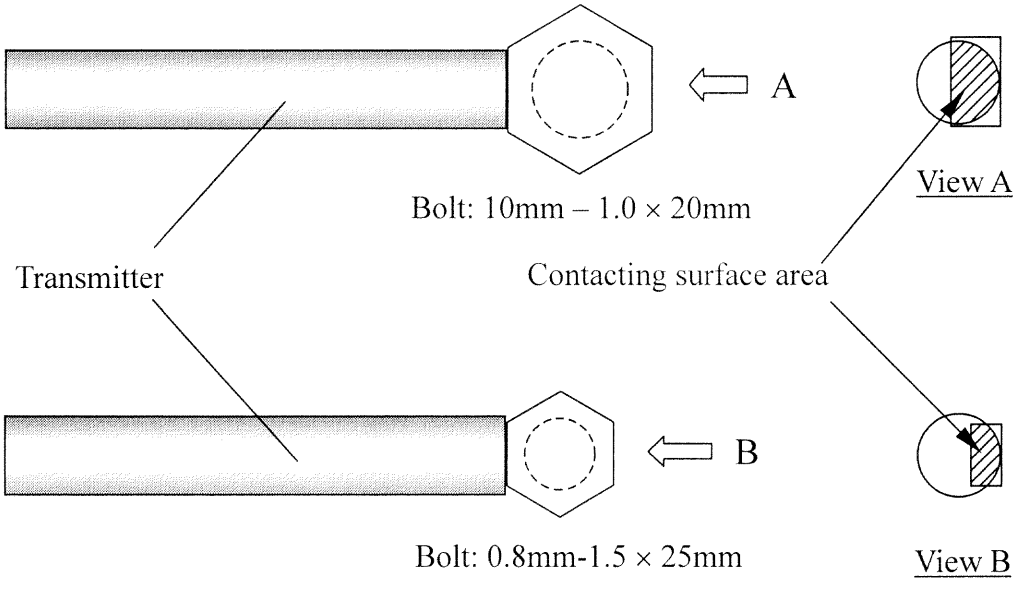

Figure 5.12 Contacting surface area is reduced in half with smaller bolt head.

5.4.2 Reflection Characteristics from a Smaller Bolt Head

Profiles of stress waves are acquired by following the procedure that was used for measuring incident wave and reflected wave in the previous experiments. Figure 5.13

shows the profiles of the incident wave and the reflected wave from a smaller bolt head. In comparison with the reflected stress wave from the larger bolt head, one noticeable difference is found at the second tensile peak. The magnitude of the second tensile peak has increased approximately 50% compare to the larger bolt head (compare with Figure 5.4). Consequently, the stress wave profile during the stable period also has shifted approximately 74mV toward tensile side compared to the stress wave profile in Figure 5.4. Therefore, the reflection ratio during this stable period (approximately, 50μs ~ 100μs) has linearly increased from –0.17 to 0.14.

When the contacting surface area between the transmitter and the bolt head is much smaller, meaning that there is a larger non-bolt-contacting surface area in the

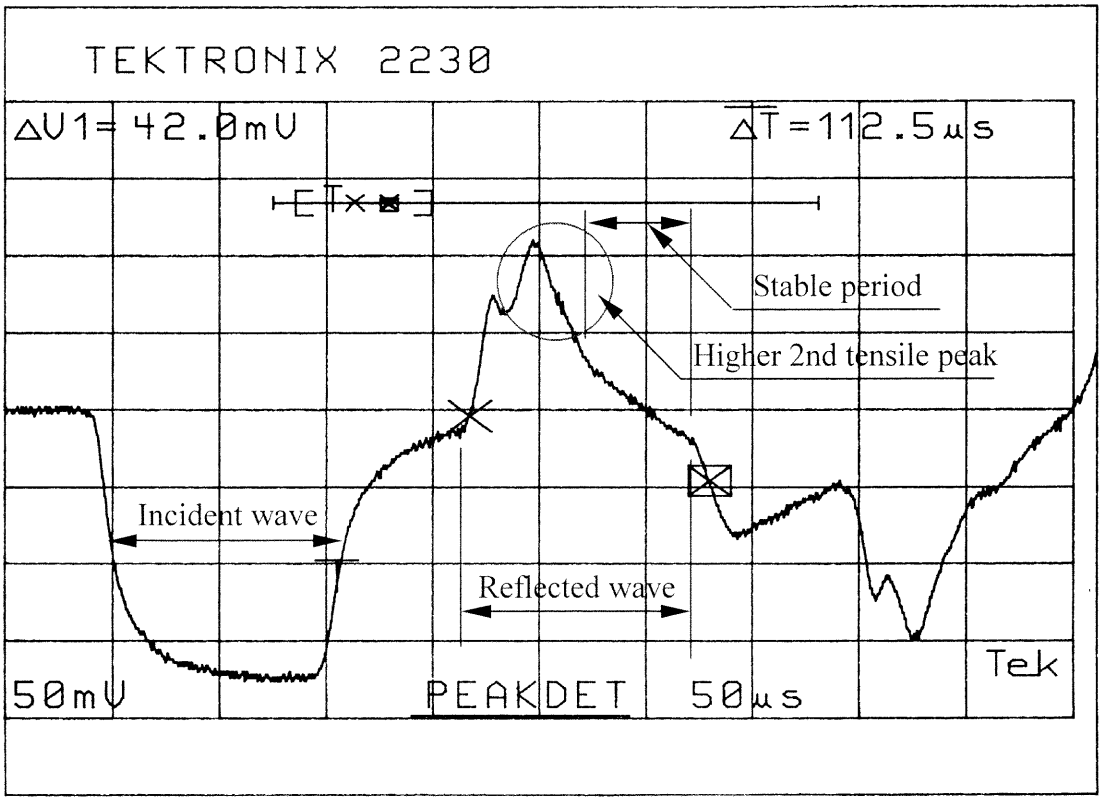

Figure 5.13 Reflection of stress wave from a smaller bolt head.

circular end of transmitter, much higher tensile peak was expected in the beginning of the reflection. It was a reasonable expectation because there is much larger free end surface from which compressive stress wave is reflected as tensile stress wave. However, as shown in Figure 5.13, the magnitude of the first tensile peak in the beginning of the reflected wave did not change compared to the first tensile peak found in the reflected stress wave from a larger bolt head (see Figure 5.4).

5.4.3 Stress Wave Profiles with a Smaller Bolt Head

First, the stress profile near the bolt-contacting end is measured by applying SRSW Method. Since the striker, transmitter and the speed of the striker are kept identical to the previous experiment with a larger bolt head, the difference in stress wave profile

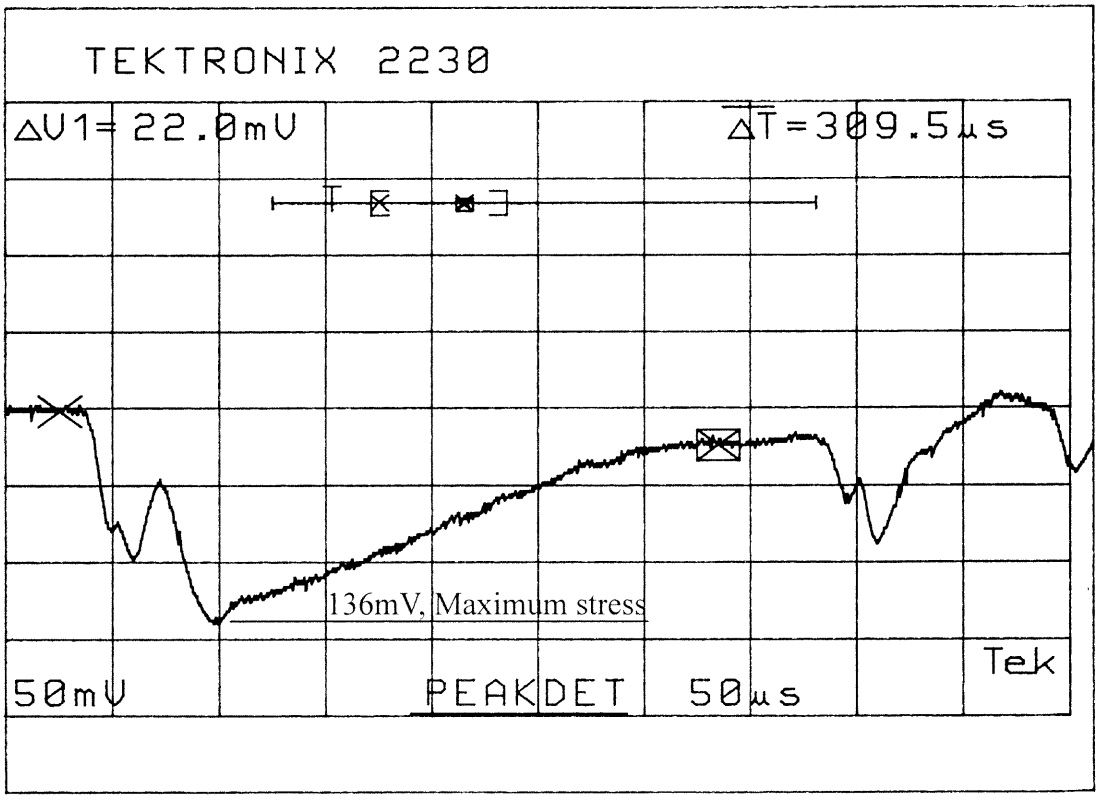

Figure 5.14 Stress at bolt-contacting end with smaller bolt head (SRSW Method).

resulted from smaller size of bolt head can be characterized. Figure 5.14 shows the measured stress profile near the smaller bolt head with SRSW Method applied. As expected form the reflection characteristics found in Figure 5.13, the magnitude of the compressive stress during the unstable period in the beginning is significantly reduced. Compared to the larger bolt head case, the location of maximum stress is shifted from the first peak to the second peak, and the time that maximum stress occurs is delayed from 30 μs to 60μs measuring from the moment of reflection. However, even with the delay in time and location of the maximum stress, its magnitude did not change much with the change of size in bolt head.

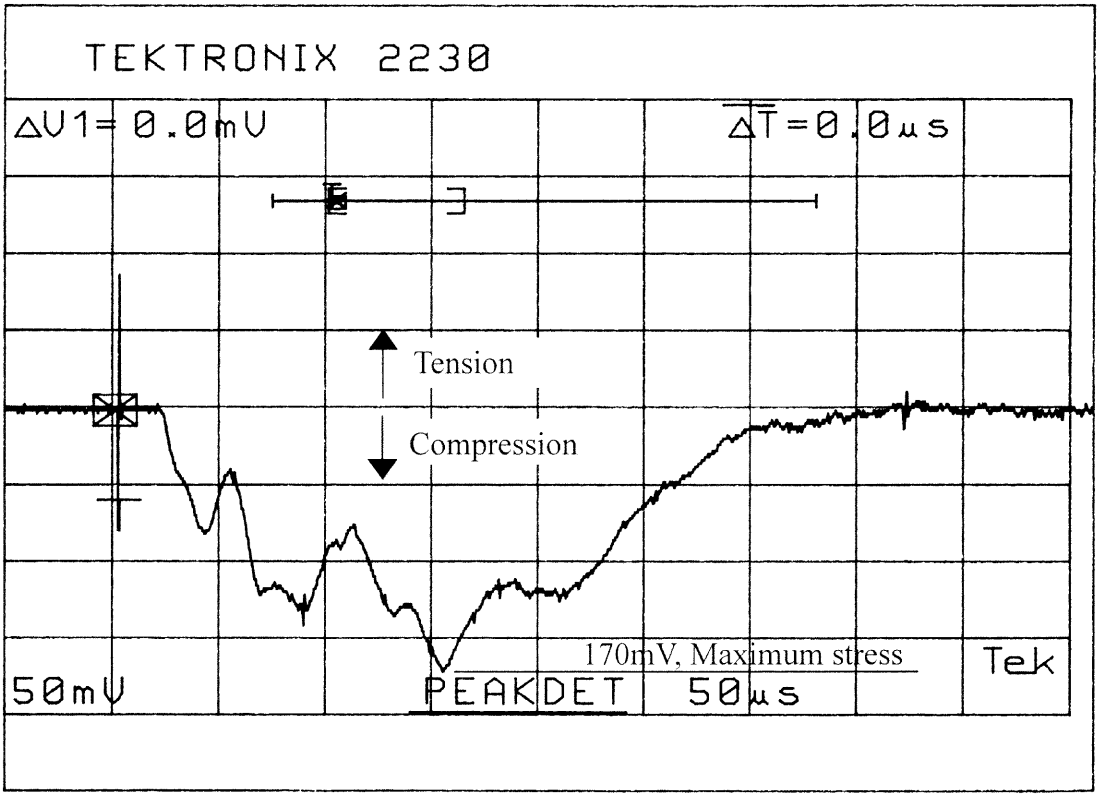

Figure 5.15 Stress at bolt-contacting end with smaller bolt head (MRSW Method).

Interestingly, the stress profiles after the unstable period (approximately 75μs from the beginning of reflection) measured in both cases are almost identical. This means that

the size of the bolt head only affects the stress profile during the unstable period not during the stable period.

One other experiment is conducted to measure the stress profile near the smaller bolt head with MRSW Method applied. Its result is shown in Figure 5.15. As expected from the reflection characteristics, the magnitude of stress in the beginning has been reduced significantly due to the increased first tensile peak found in the beginning of the reflected wave. It is noticeable in Figure 5.15, compared to the stress profile shown in Figure 5.16 obtained with a larger bolt head, that the magnitude of periodic compressive stress have been reduced in the first two periods. However, as time lapses, the compressive stress near the bolt-contacting surface is increased and reached to the maximum stress as much as in the experiment with a larger bolt head.

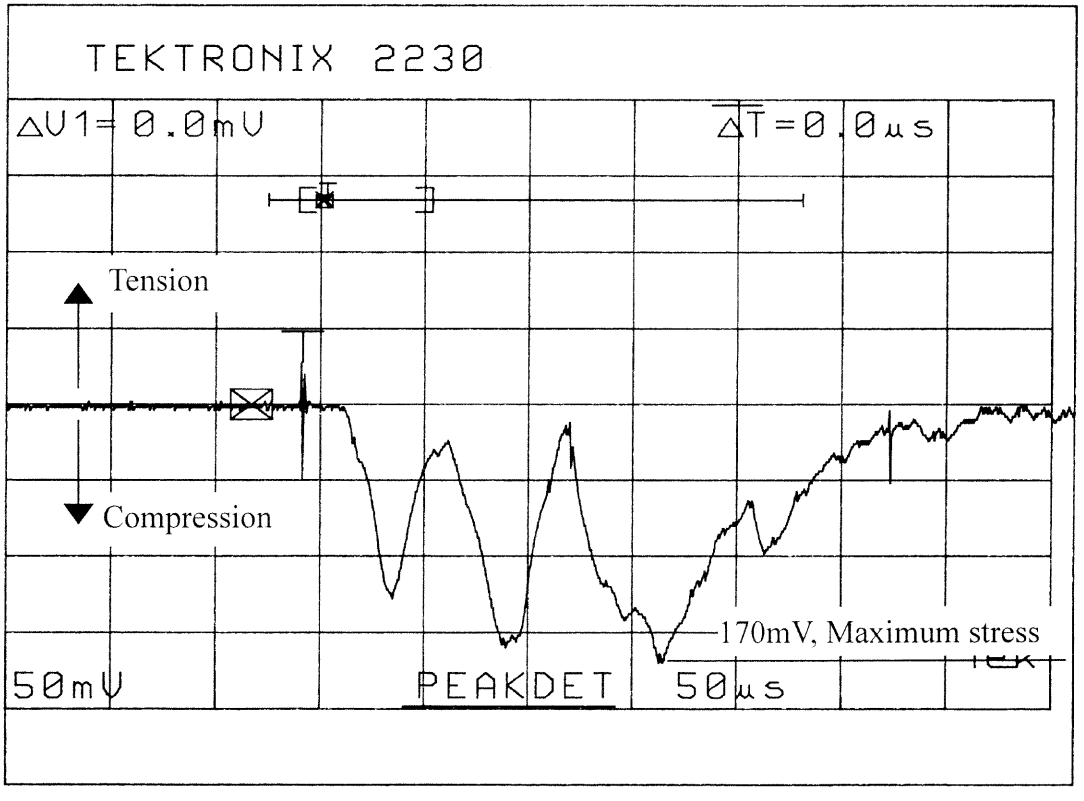

Figure 5.16 Stress at bolt-contacting end with larger bolt head (MRSW Method).

5.4.4 Efficiency of MRSW Method with a Smaller Bolt Head

It seems from the experiment with a smaller bolt head that the size of bolt head affects the stress profile only in the beginning (unstable period). The experiment obtaining the reflection characteristics shows that a smaller bolt head causes the second tensile peak becomes much higher in tensile direction. Consequently, it reduces the compressive stress at the bolt-contacting surface in both SRSW Method and MRSW Method is applied. Although the location of the maximum stress is shifted in SRSW Method, its magnitude reached as much as in the experiment with larger bolt head. In both cases of MRSW and SRSW Methods, the magnitudes of maximum stress were not affected by the size of bolt head. Therefore, the efficiency of increasing the maximum stress applying MRSW Method to a smaller bolt head remains same as it is to a larger bolt head.

5.5 Consistency of the Experimental Results

The experimental results presented in this chapter, including the reflection characteristic profile and the stress wave profiles obtained with SRSW and MRSW Methods, are chosen from ten repetitive results for each experiment. In each experimental subject, the results were consistent throughout the repeated experiment with little variation in noise. The presented experimental results represent the average of the ten repetitive results for each experiment.

CHAPTER 6

DISCUSSION AND APPLICATION IN PRODUCT DISASSEMBLY

In an attempt to improve the efficiency of destructive disassembly process, fracturing bolt head using mechanical impact has been introduced. The impact stress waves in a mechanical arrangement for fracturing bolt head are studied, and a new technique that creates higher maximum stress on a bolt neck is proposed. The equations are developed to provide a theoretical basis of the proposed technique. However, the unique characteristic found in the stress wave profiles that was reflected from a bolt head made the analysis deviate from experimental results. This unique characteristic of a bolt head in response to a dynamic impact worked as a negative factor in both conventional (SRSW) and new (MRSW) methods. It caused the maximum stresses to be reduced and become much less than they are expected in analysis. Meanwhile, even with this negative characteristic, the relative evaluation of both methods with the experiments showed that the proposed method generates higher stress with the same amount of energy invested in launching the striker.

In this chapter, some of the factors that affected the analysis and the experiments are discussed. Then potential application of the new technique in a destructive disassembly process is addressed along with the proposal of future studies.

6.1 Discrepancies between Analysis and Experiment

6.1.1 Positioning Problem of Strain Gauges

Measuring stress waves at the interfacing surface between bolt head and transmitter is not an easy task. In many cases, load cells are widely used to measure static and dynamic mechanical loads. But placing a load cell in between them and measuring stress waves with it would not be a proper technique for the experimental purpose because the load cell itself will cause interference in transmitting stress waves between bolt and transmitter. Instead, stress waves are measured in the experiment with a pair of strain gauges attached to the transmitter bar near the bolt-contacting end in order to avoid influence from

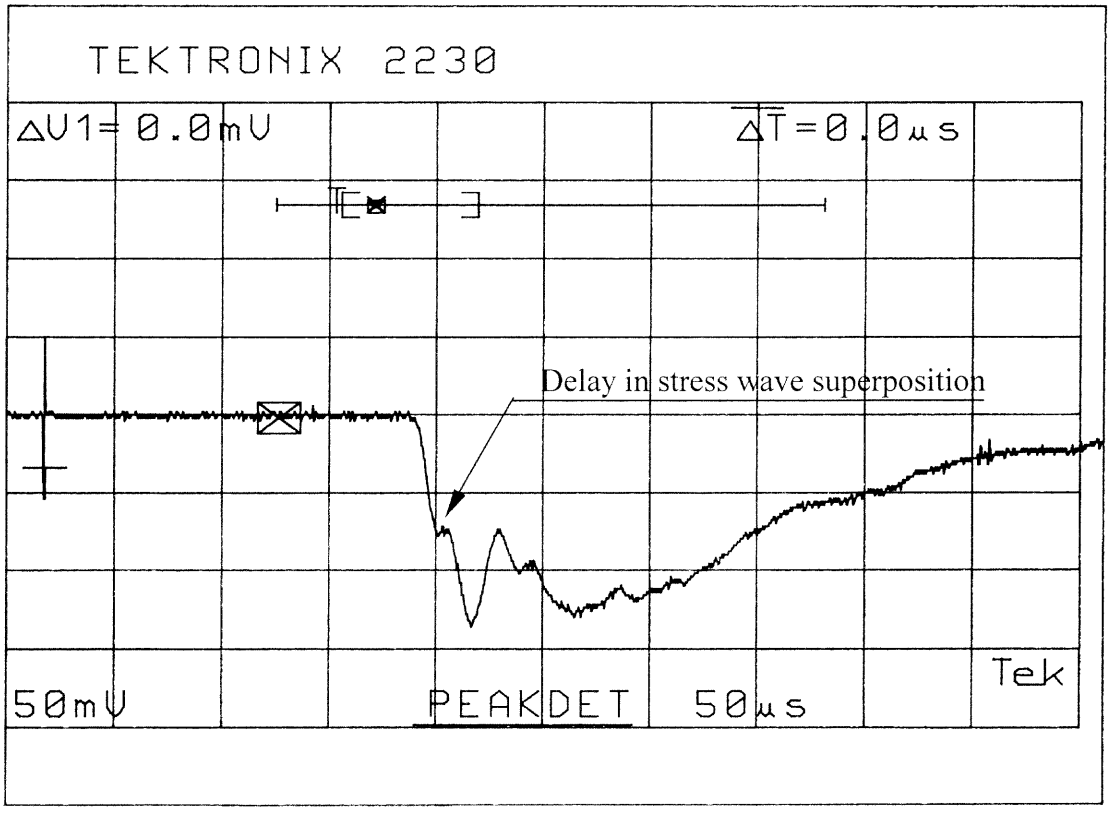

Figure 6.1 Delay in stress wave superposition due to the positioning problem of strain gauges.

measuring devices. This method of measuring stress waves has been used in many other researches studying elastic stress waves in one-dimensional bars. However, the strain gauges were attached only near to the bolt-contacting surface, because if they were too close, they would give us distorted signals with noise. For this reason, the stress waves can be measured near the bolt-contacting end, not at the bolt-contacting surface. Therefore, the stress wave profiles acquired from this set of strain gauges cannot be an accurate measurement to be compared with the analytic solution for the stress wave

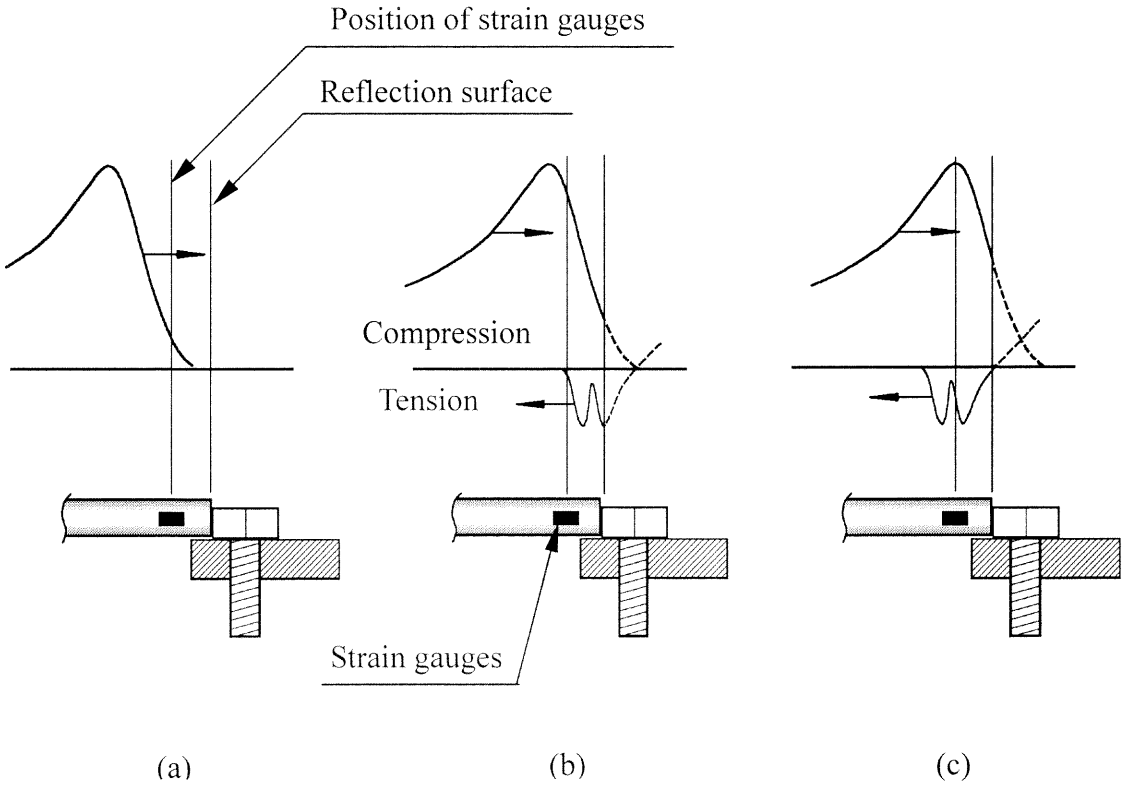

Figure 6.2 Graphic illustration of delay in stress superposition.

profiles at the bolt-contacting surface. In Figure 6.1, the delay in stress wave superposition during the first 20μs near the bolt-contacting end is resulted from this strain gauge positioning problem. This effect of delay in stress wave superposition is

illustrated in Figure 6.2. The striker impinges on one end of the transmitter and generates compressive stress wave that will travel along the transmitter bar. When the stress wave travels toward the bolt-contacting end, it passes the strain gauges right before it reaches to the contacting surface (Figure 6.2a). The measured stress continues to rise until the wave front that reflected from the bolt head comes back to the strain gauges again (Figure 6.2b). From this moment, superposition between the compressive stress wave coming from the struck end and the reflected tensile wave occurs at the position of strain gauges. However, when the stress wave comes back from the reflection, its shape has been changed due to the 'unstable period' found in the beginning of the reflected wave from a bolt head. Then the two tensile peaks in this 'unstable period' of reflected wave pass through the strain gauges (Figure 6.2c). If the strain gauges are attached closer to the interfacing surface, the effect of delay in stress wave superposition will be reduced. However, if the strain gauges are too close to the interfacing surface, the possibility of getting distorted waves and noise increases.

If the purpose of the experiment were to measure the stress wave profiles exactly at the bolt-contacting surface and to evaluate them with the analytic solution, it would be needed to adopt other technique more precisely designed for that purpose. However, the measurements in this experiment are aimed at relative evaluation between the experimental results acquired by applying different methods. Thus, as long as the strain gauges are attached at the same distance from the bolt-contacting end for both methods, the position of the strain gauges seems acceptable for the experimental purpose of this research.

6.1.2 Contact Condition between Transmitter Bar and Bolt Head

One of the factors that affected the accuracy of experimental results is related to the initial state of contact between the transmitter bar and the bolt head. This factor was not considered in developing the equations. It was assumed that the entire circular surface at the end of the transmitter bar is in full contact with the bolt head while the stress waves are being reflected. However, even with a considerable effort to increase the initial contact surface area, this condition was difficult to realize in this experiments.

Meanwhile, it has been observed that the duration and its magnitude of the first tensile peak in the reflected stress wave get shorter and smaller respectively as the initial contact surface gets larger. The shorter duration of the first tensile peak, which was

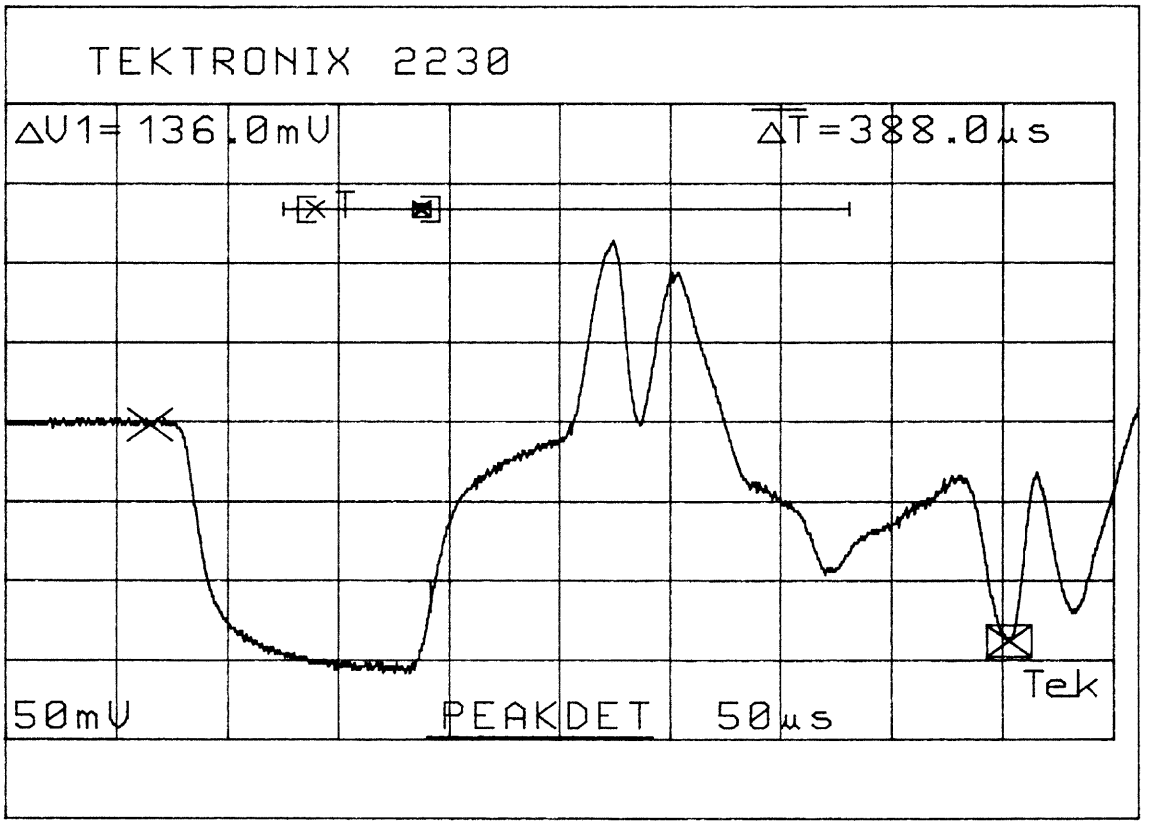

Figure 6.3 Higher and longer tensile peaks due to a poor initial contact.

caused by a better contact condition, resulted in increasing the maximum stress in both SRSW Method and MRSW Method.

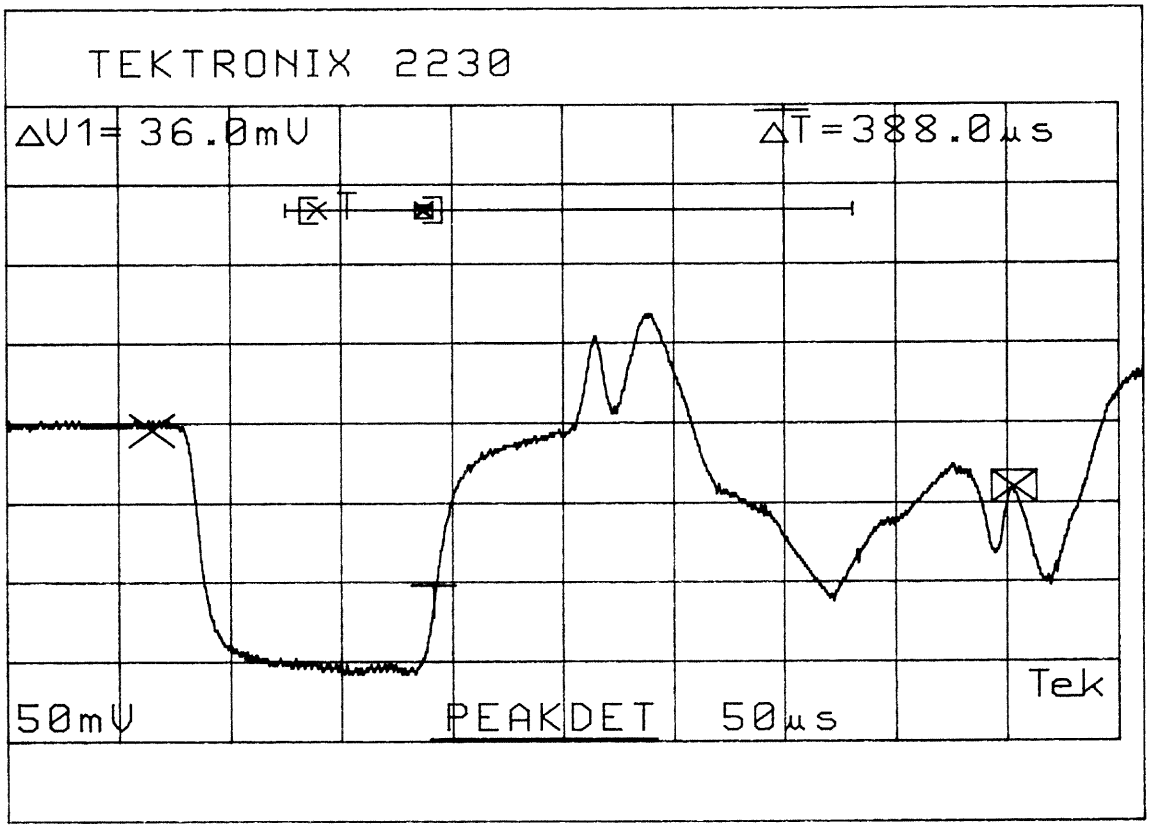

Figure 6.4 Lower and shorter tensile peaks due to a better initial contact.

6.1.3 Elasticity of Striker

The assumption made for the striker as rigid could have caused the discrepancy between the analysis and the experimental result especially on MRSW Method. In the analysis, the striker was assumed rigid. However, the striker in the experiment is made of steel as the transmitter bar, and they are elastic. Therefore, in the analysis of MRSW Method, while the stress wave travels back and forth between the struck end and the bolt-contacting end, some of the stress wave transmits into the striker and loses its energy. This phenomenon would have affected actual stress wave profile become lower than the stress wave profile obtained from the analysis starting from the second period.

6.1.4 Damping Effect of Transmitter Bar

When stress wave travels through a section of transmitter bar, it causes longitudinal and radial motions of expansions and contractions in that section. These motions create internal friction and consequently, the stress wave loses its energy and attenuates as it travels along the transmitter bar. Usually, this phenomenon is said to be a damping effect. In the report presented by Studny et al [36], this damping effect was considered as they calculate the fracture energy of a screw head. The damping was an appreciable amount of effect when they calculate the fracture energy by comparing the incident wave and the reflected wave returning after fracturing a screw head. However, this damping effect was not taken into the consideration in the analysis since it has much less influence than other factors in this relative evaluation of experimental results. The damping effect was not a significant factor in this relative evaluation of actual maximum stresses generated by different methods.

6.1.5 Non-Constant Characteristics of Reflection Ratio *R*

The analytic equations developed in this research are based on the assumption that stress waves reflect from a bolt head with a constant ratio. This assumption might be true if the transmitter is in contact with an elastic object with no abrupt change in its geometry near the interfacing surface between the transmitter and the object. In the experiment,

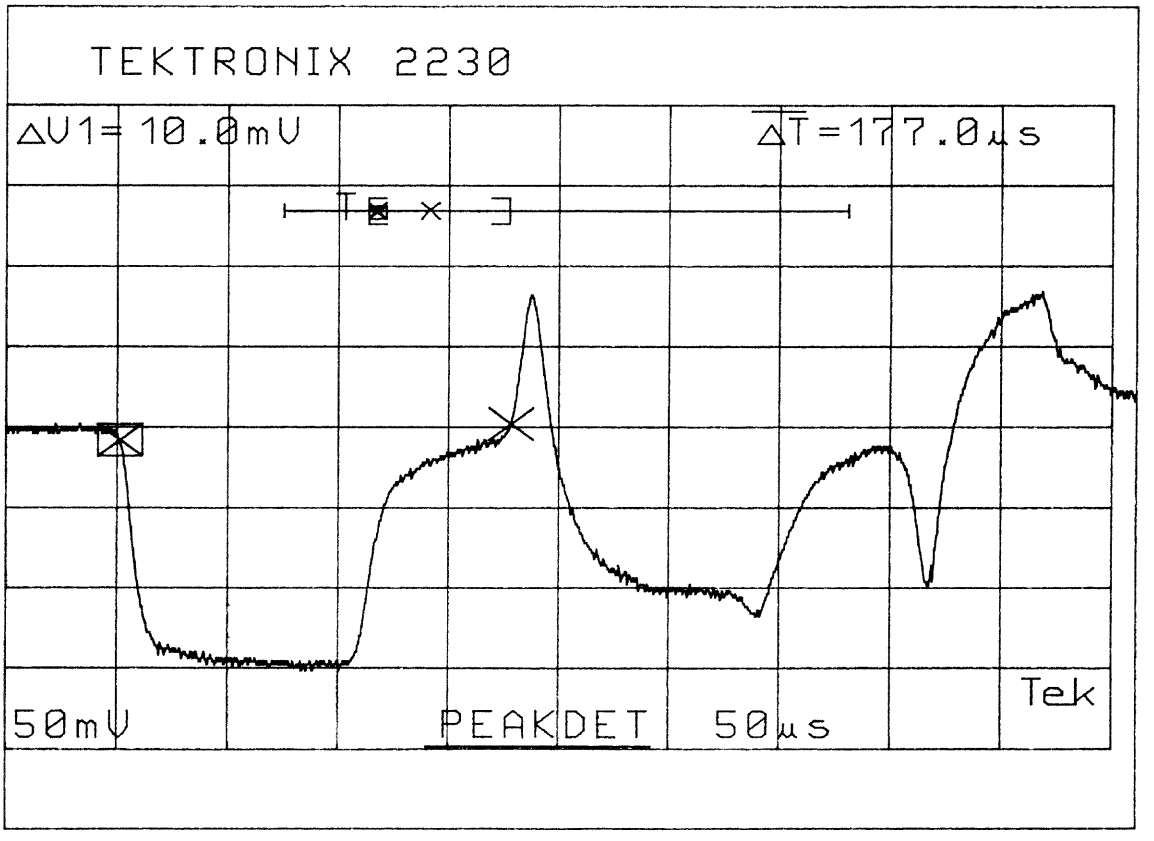

Figure 6.5 Reflection of stress wave showing constant reflection magnitude.

when the transmitter is in contact with an edge of the angled beam assembly, it is observed that the magnitude of reflected stress wave remained in a constant value (see Figure 6.5). If it were not for the tensile peak resulted from the initial contact condition, the assumption made for *R* being constant is reasonable in this situation. However,

when the transmitter is in contact with a bolt head, the reflected stress wave shows very complex characteristics. Therefore, the assumption made for R in this case is not appropriate in order to predict an exact solution of the stress wave profiles.

6.1.6 Extension of Time Intervals between the Peaks

One noticeable phenomenon found in the experiment of MRSW Method is that the time intervals between the peaks are longer than they are expected in the analysis. In the analysis, the time required for the stress waves make a round trip up and down the transmitter is 40μs (c_L = 5150m/s, l_t = 103mm). This length of time interval should be equal between the peaks. However, the experiment shows that the time intervals

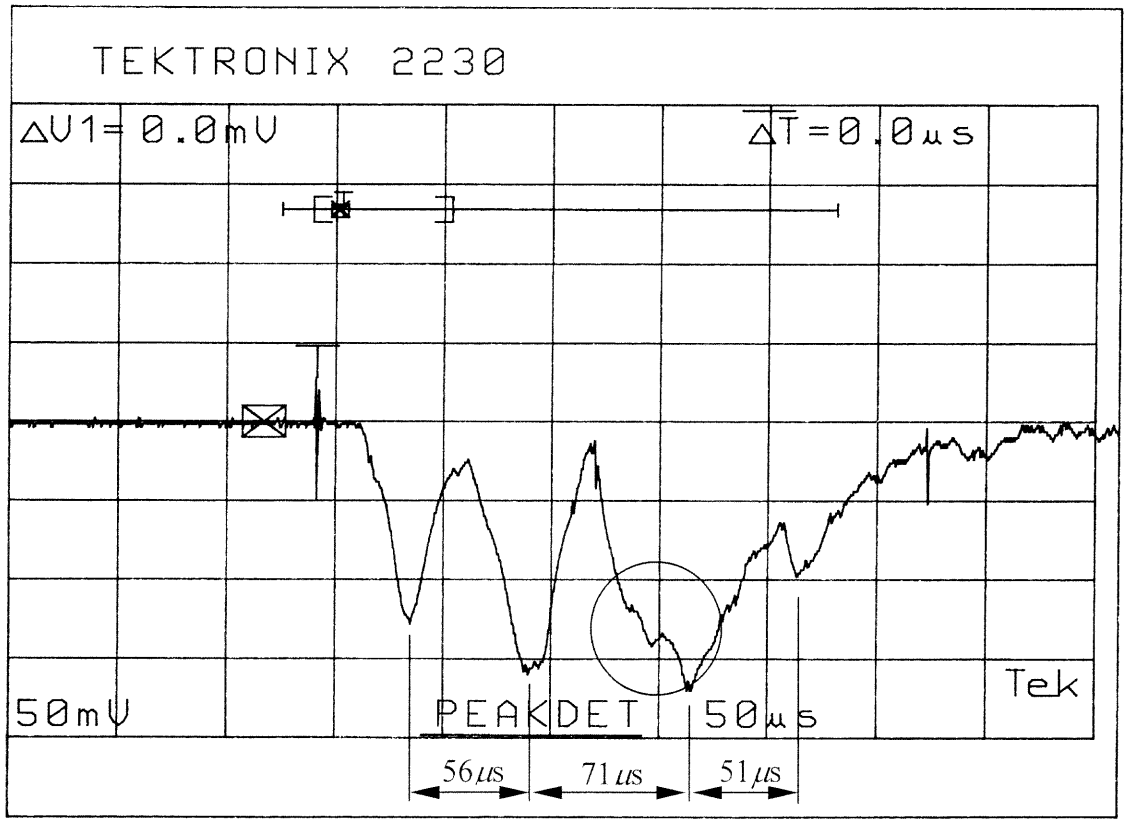

Figure 6.6 Experimental result of MRSW Method showing irregularity in time intervals between the peaks.

between the peaks are longer than the ones in the analysis. In addition, it is also observed that the lengths of the time interval between consecutive peaks are different from each other. At this point, it is not certain from the experiment what caused this phenomenon, and there was no literature found that addresses these issues. Meanwhile, it seems that some type of disturbance affects the stress wave profile at the third peak and therefore the location of the maximum stress is shifted from its original location. Therefore, the lengths of the time intervals between the peaks become irregular. This disturbance might be the tensile stress waves returned from edges on the other side of the angled beam assembly.

6.2 Application of MRSW Method in Destructive Disassembly

When the equations for the stress waves in MRSW Method are developed, the geometrical aspect of a protruded bolt head was not accounted. The assumption made for the transmitter in contact with a bolt head is equivalent to the situation in that the transmitter is in contact perpendicularly with an elastic half space. Therefore, in order for the exact evaluation of the equations developed for MRSW Method, an experimental setup similar to the one developed by S. Boucher and H. Kolsky [43] would be needed. However, since the experimental purpose is to show the feasibility of applying MRSW Method in destructive disassembly to increase energy efficiency, the experiments are conducted with an emphasis on a relative evaluation between the two methods. Moreover, it is shown in the experiments that the maximum stress reaches higher with MRSW Method than with a conventional SRSW Method. Therefore, if more information about the reflection characteristics were gathered from different sizes and types of bolt corresponding to different types of mounting material and structure, it would

be useful for design purposes of a destructive disassembly device. In designing a disassembly device, when dynamic strength for fracture of the bolt is given, physical parameters of striker and transmitter can be determined based on the reflection characteristics.

Modifications can be made to improve the performance of disassembly device. Among them, it is possible to modify the shape of the end of the transmitter that contacts bolt head in order to improve contact condition or to increase the stress exerted on a bolt head. Modifying the transmitter bar by shaping its end into a chisel type profile may produce higher stress to a bolt head. However, stress waves become highly distorted when they reflect from this type of end [36]. Therefore, modifying the end into a chisel type may give good results in actual practice, but is not useful for the experimental purposes of this research.

CHAPTER 7

CONCLUSIONS AND RECOMMENDATIONS FOR FUTURE WORK

7.1 Contribution to Destructive Disassembly

The objective of this research was to present a new method for improving the efficiency of destructive disassembly processes. The type of destructive disassembly in this research consisted of breaking a protruded bolt head by applying side impact, which is proven to be feasible and applicable as a rapid and cost effective disassembly method. This research adopted and modified the classical analysis of stress waves in one-dimensional bar, and developed a method to improve the efficiency of generating stresses on the bolt head. The classical analysis provides the stress wave equations in one-dimensional bar that has its end attached to an infinite rigid mass. However, in most disassembly situations, the medium or the structure on which the bolt is mounted cannot be treated as rigid. Therefore in the analysis, the equations for the stress waves are developed based on the assumption that this end of the bar is attached to an elastic medium. In other words, it was assumed that there exists a ratio in magnitudes between the stresses before and after the reflection. The developed equations and their analysis provide the time histories of non-dimensional stresses at both end of the bar for different values of reflection ratio and mass ratio between the bar and the striker.

Experiments for precise evaluation of the developed equations can be conducted with a transmitter bar that has its end attached to an infinite elastic half space. However, the objective was to show feasibility of the new method, and the experiments in this research were conducted focusing on the relative evaluation of maximum stresses between the conventional and the new methods.

The reflection characteristics of stress waves from a bolt head were unique, and they are more complex than that from an elastic half space. These unique characteristics from a bolt head caused discrepancies between the stress wave profiles obtained from the experiment and the analysis. Even though, as expected in the analysis, the maximum stress was increased in the experiment with the new method. Therefore, it was shown that with the new method the stress exerted on a bolt head could be increased with the same amount of energy invested on the striker. This research made the following contributions:

1. This research developed the equations representing stress waves in one-dimensional bar caused by impact when the bar is in contact with a bolt head mounted on an elastic medium. The developed equations provide the understanding of impact mechanism involved in the process of fracturing a bolt head by applying side impact.

2. Based on the developed equations, this research developed the equations representing the shear stress at the neck of joining element for both cases of single reflection and multiple reflections.

3. This research developed a new method that generates higher shear stress at the neck of joining element without increasing the energy input to striker. This research provided the analysis showing that the developed method creates higher stress at the neck of joining element than applying conventional method.

4. This research provided the experimental results supporting the analysis and the feasibility of the new method. The experiments showed that the stress waves reflecting from a bolt head have very unique characteristics, and they cause the stress

profiles acquired from the experiment deviate from the analytic results.

5. This research improved the efficiency of applying mechanical impact to fracture joining elements by introducing the new method.

7.2 Recommendations for Future Work

Analysis of materials or structures under impact loads involves much more complicated problems than dealing with static loads. One of the reasons is that when impact is applied to an object, it introduces stress waves and vibrations into the objects, which are time-dependant, and involves mathematical issues. Then the results of analysis become highly sensitive to small changes of parameters or boundary conditions. The stresses resulting from impact depend upon many parameters such as: the shape and mass of the struck body and the striking body, the relative striking speed or force, and the physical properties of the materials [44], and etc. Likewise, the mechanical arrangement introduced in this research may have some parameters, which are not included in the analysis but have significant effect on the result of actual implementation. For example, the initial contact condition between the transmitter and the bolt head, which is not accounted in the analysis, affected the maximum stress in both SRSW and MRSW Methods. It would be very difficult to maintain consistency of this condition if the initial contact is made manually in a fast moving disassembly line. However, it is not certain how much the initial contact condition would affect the maximum stress in both methods. The influence of contact condition might be negligible if the speed of striker is very high. It is also of interest how the tensile peaks in the beginning of the reflected wave would affect the stress wave profile in both methods with a higher speed of striker.

One of the parameters that need to be considered in the actual implementation is the angle of contact between the bolt and the transmitter. The impact is applied perpendicularly to the bolt head in the experiment, which is obviously the best way to maximize the shear stress in the bolt head. However, in practice, it also would be difficult to maintain this condition. In some situation, in order to improve accessibility and contact condition, the bolt-contacting surface of the transmitter can be modified to have the best contact with a bolt head by shaping it with an angle. The influence from different angles of contact needs to be assessed for practical implementation.

The reflection characteristics to the combinations of different sizes of bolt and different types of bolt-mounting body and their influence to the stress wave profiles in both methods need to be characterized. When bolt is mounted on a soft material or a soft structure so that the reflection ratio is small, MRSW Method would not be effective. If the reflection ratio is too small, which means the stress wave loses too much of its energy to the bolt-mounting body the magnitude of the stress at the bolt-contacting end would not rise as much from the second period. In this case, the situation also would not be favorable to SRSW Method because the energy of stress wave would be dispersed into the bolt-mounting body before it builds shear stress at the bolt neck. In an extreme, the impact will cause fracture at the bolt-mounting body instead of breaking the bolt head. Therefore, it would be useful to have the criteria for bolts and bolt-mounting bodies whether they are eligible for MRSW Method to be effective. These requirements can be established with the bolt size and its fracture strength to dynamic impact related to the material properties and structural characteristics of the bolt-mounting body.

APPENDIX

PHOTOGRAPHS OF THE EXPERIMENTAL SETUP AND EQUIPMENTS

The followings show the experimental setup and equipments described in Chapter 5.

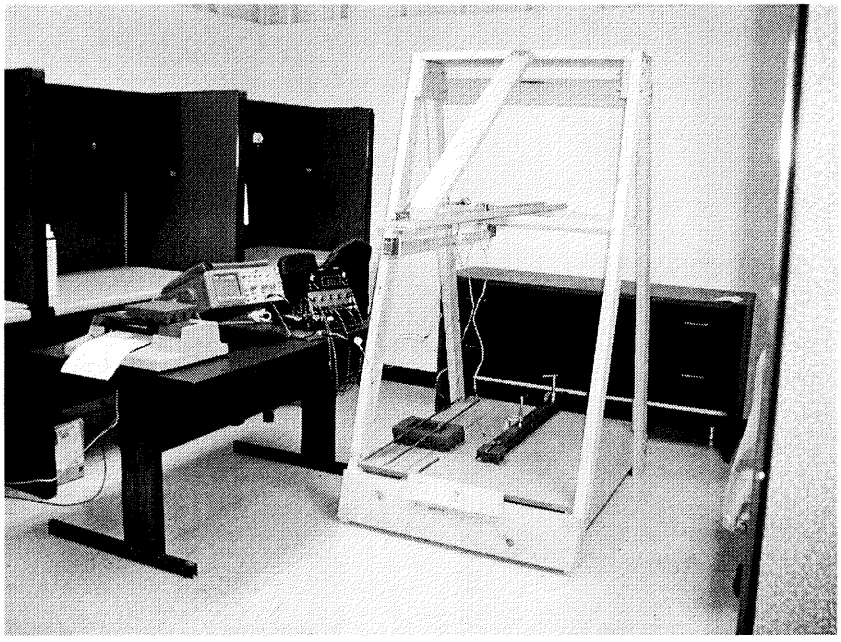

Figure A.1 Experimental setup.

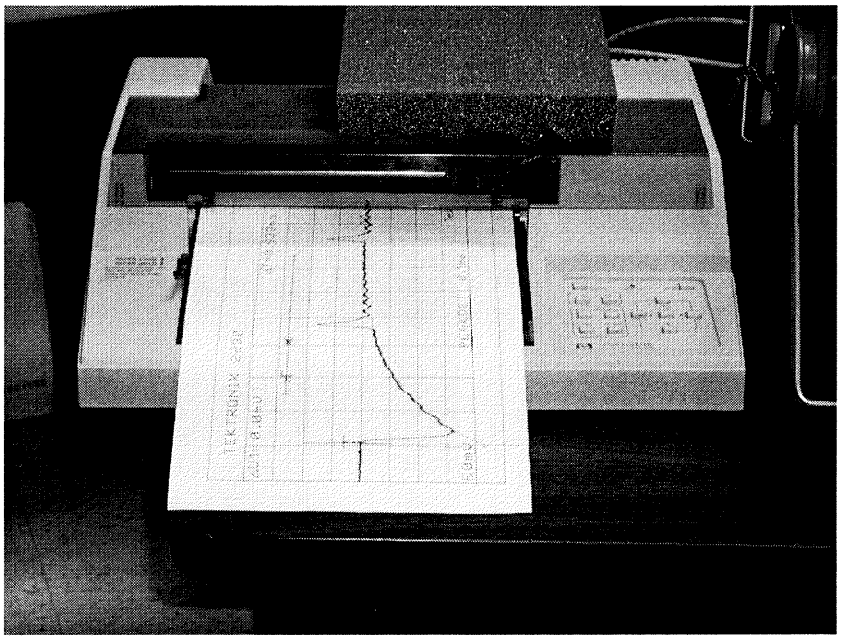

Figure A.2 Pen plotter, HP4470A.

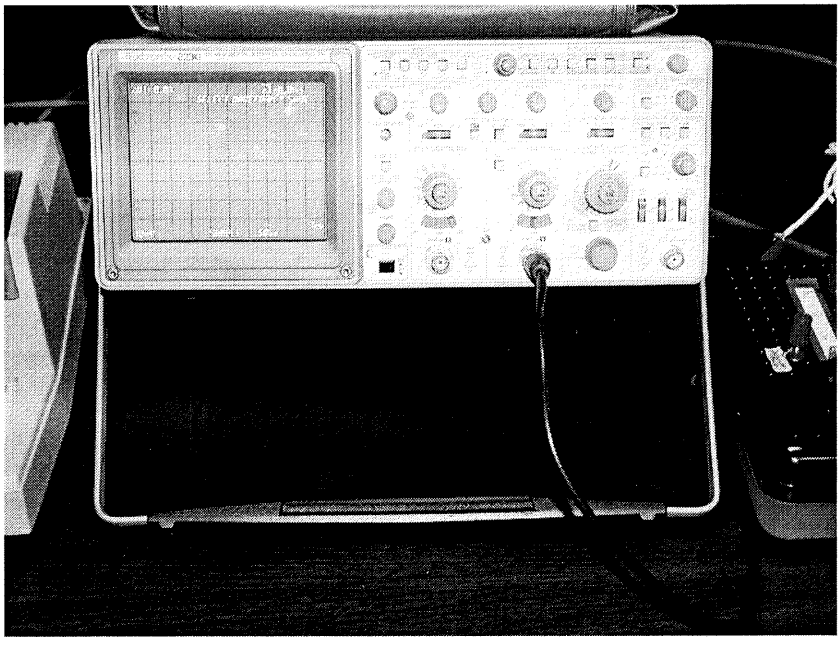

Figure A.3 Oscilloscope, Tektronix 2230.

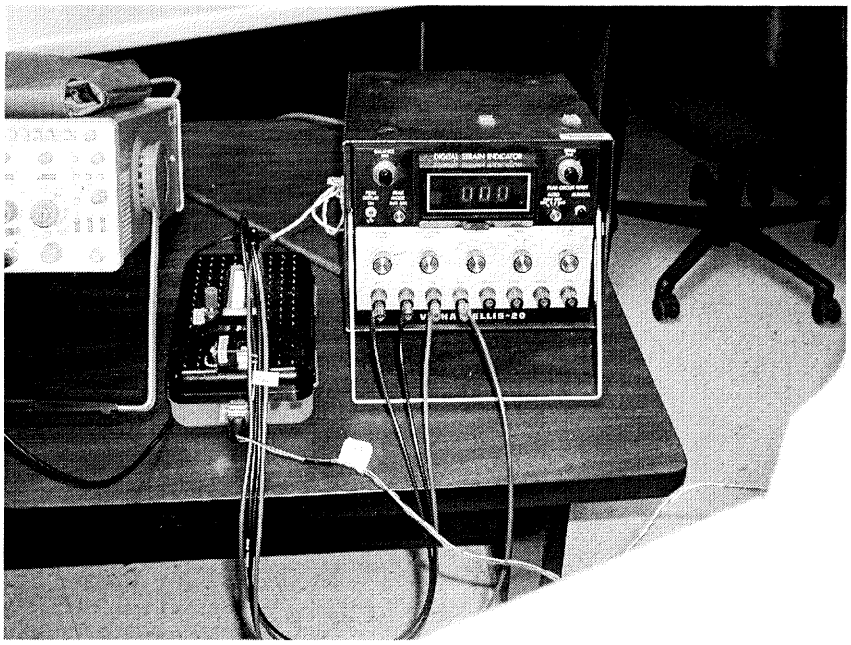

Figure A.4 Bridge box and strain amplifier, VISHAY ELLIS-20.

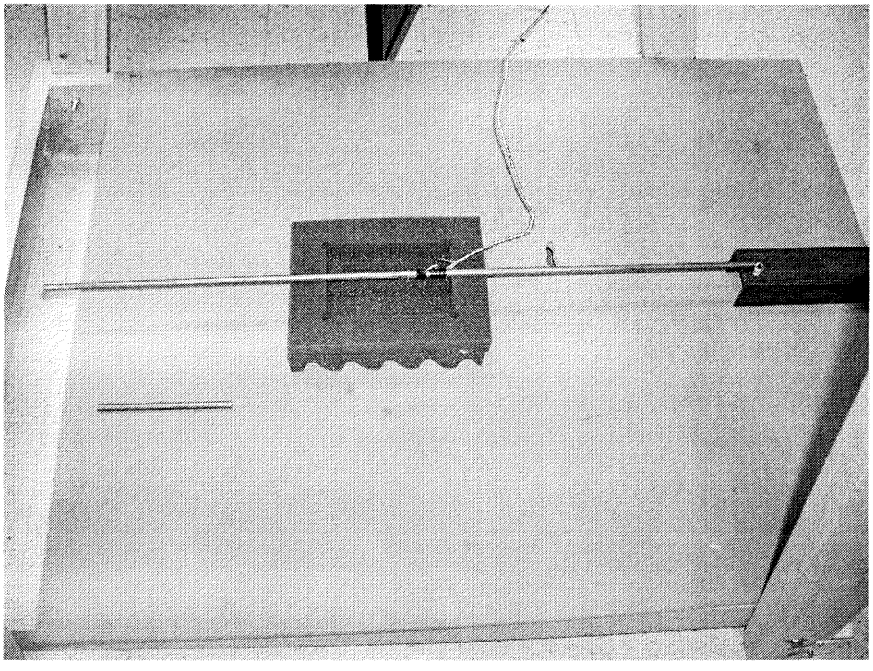

Figure A.5 Transmitter for measuring reflection characteristics and striker.

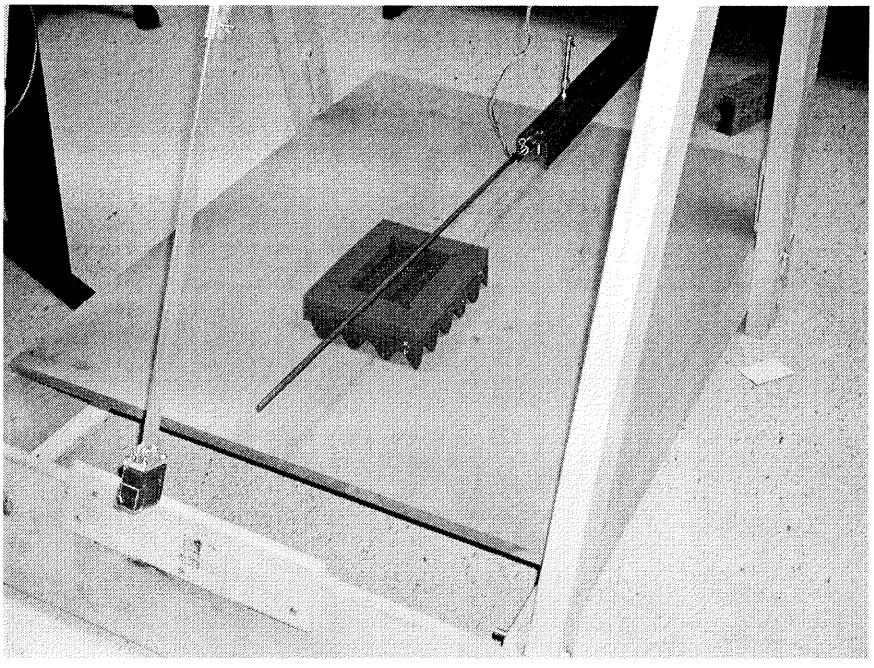

Figure A.6 Striker hitting transmitter in SRSW Method.

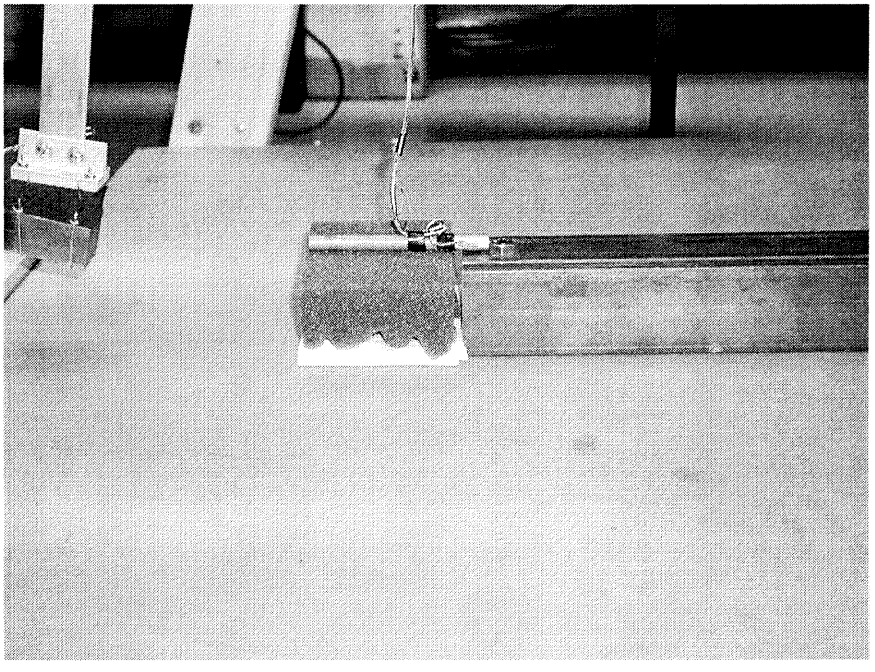

Figure A.7 Striker hitting transmitter in MRSW Method.

REFERENCES

[1] Hari Srinivasan, N.Shyamsundar and Rajit Gadh, "A virtual disassembly tool to support environmentally conscious product design", IEEE, 1997.

[2] Henstock M., "Design for Recyclability", The Institute of Metals, 1988.

[3] Chen R., Navin-Chandra, and Prinz F., "Product design for recyclability; a cost benefit analysis model and its application", IEEE International Symposium on Electronics and the Environmental, 1993.

[4] Kirby J. and Wandehra I., "Designing business machines for disassembly and recycling", IEEE, 1993.

[5] Noller R., " Design for disassembly tactics", Assembly Journal, 1992.

[6] Gupta S. M. and McLean C R, "Disassembly of Products", Computers and Industrial Recycling, V1-2, pp. 225-228, 1996.

[7] Penev K. D. and Ron A. J., "Determination of a disassembly strategy", International Journal of Production Research, V34, No.2, pp. 495-506, 1996.

[8] Hrinyak M., Bras B. and Hoffman W. F., "Enhancing design for disassembly; a benchmark of DFD software tools", Proceedings of the ASME DET and CIE Conference, 96-DETC/DFM-1271, 1996.

[9] Shyamsunder N., Ashai Z. and Ghad R., "Virtual Design for disassembly methodology", Journal of Engineering Design and Automation, 1996.

[10] Vigon, B. W. and Curran, M. A., "Life Cycle Improvements Analysis: Procedure Development and Demonstration", Proceedings of IEEE International Symposium on Electronics and the Environment, pp. 151-156, 1993.

[11] Tummala, R. L. and Koenig, B. E., "Models for Life Cycle Assessment of Manufactured Products", Proceedings of IEEE International Symposium on Electronics and the Environment, pp. 94-99, 1994.

[12] Veldstra, M. and Bouwa, T., "Environmentally Friendly Design in Plastics", Proceedings of the 9th International Conference on Engineering Design, No. 2, pp. 820-826, 1993.

[13] Vigon, B. W., and Curran, M. A., "Life Cycle Improvements Analysis: Procedure Development and Demonstraion", Proceedings of IEEE Internatinal Symposium on Electronics and the Environment, pp. 151-156, 1993.

[14] Tummala, R. L. and Koenig, B. E., "Models for Life Cycle Assessment of Manufactured Products", Proceedings of IEEE International Symposium on

Electronics and the Environment, pp. 94-99, 1994.

[15] Veldstra, M. and Bouwa, T., "Environmentally Friendly Design in Plastics", Proceedings of the 9th International Conference on Engineering Design, No. 2, pp. 820-826, 1993.

[16] Hanft, T. A., and Kroll, E., "Ease of Disassembly Evaluation in Design for Recycling", Design for X-Concurrent Engineering Imperatives, Huang, G. Q., ed., Chapman & Hall, 1995.

[17] Emblemsvag, J. and Bras, B., "Activity Based Costing in Design for Product Retirement", Proceedings of 20th Design Automation Conference, ASME DE-Vol.69, pp. 351-361, 1994.

[18] Zussman, E., Kriwet, A. and Seliger, G., "Disassembly–Oriented Assessment Methodology to Support Design for Recycling", Annals of the CIRP, V43, pp. 9-14, 1994.

[19] Navin-Chandra, D., "ReStar: A Design Tool for Environmental Recovery Analysis", Proceedings of the 9th International Conference on Engineering Design, No.2, pp. 780-787, 1997.

[20] Yoshimura Masataka, "Design Optimization for Product Life Cycle", Design for X-Concurrent Engineering Imperatives, by Huang, G. Q. (ed) Chapman & Hall, pp. 429-440, 1995.

[21] Das, S. K., Yedlarajiah, P. and Narendra, R., "An approach for estimating the end-of-life product disassembly effort and cost", International Journal of Production Research, 2000.

[22] Knight, W. A. and Boothroyd, G., "Analysis of Products for End-of-Life Management", IEEE, 1997.

[23] Dowie, T. and Kelly, P., "Estimation of disassembly times," Unpublished Technical Report, Manchester Metropolitan University, United Kingdom, 1994.

[24] Kroll, E., "Application of work-measurement analysis to product disassembly for recycling," Concurrent Engineering Research and Applications, Vol.4(2), pp. 149-158, 1996.

[25] Kroll, E., Beardsley, B. and Parulian, A., "A methodology to evaluate ease of disassembly for product recycling," IIE Transactions, Vol. 28, pp. 837-845, 1996.

[26] Subramani, A. and Dewhurst, P., "Automatic generation of product disassembly sequences", Annals of the CIRP, 1991.

[27] Gershenson, J. and Ishii, K., "Life-cycle serviceability design", ASME Design Theory and Methodology, 1991.

[28] Brayan C., Eubanks C. and Ishii K., "Data representation for serviceability design", ASME Design Theory and Methodology, 1992.

[29] Laperriere L. and Elmaraghy H., "Planning of products assembly and disassembly", Annals of the CIRP, 1992.

[30] Seliger, G., Hentschel, C. and Wagner, M., "Disassembly Factories for Recovery of Resources in Product and Material Cycles", Proceedings, Prolomat '95, F-L Krause ed, Berlin, Germany, pp. 58-67, 1995.

[31] Zimmermann, H. J., "Fuzzy Set Theory and its Applications", Kluwer Academic Publishers, Boston, 2nd Edition, 1991.

[32] Hentschel, C., Seliger, G. and Zussman, E., "Grouping of Used Products for Cellular Recycling Systems", Annals of the CIRP, Vol.44, pp. 11-14, 1995.

[33] Feldmann, K. and Meedt, O., "Recycling and Disassembly of Electronic Devices." Proceedings, Prolomat '95, F-L. Krause, ed., Berlin, Germany, pp. 233-245, 1995.

[34] J.D. Chiodo, E.H. Billett and D.J. Harrison, "Active Disassembly Using Shape Memory Polymers for the Mobile Phone Industry", International Symposium on Electronics & the Environment, pp. 151-156, May 1999.

[35] Studny, D., Rittel, D., Zussman, E. "Impact Fracture of Screws for Disassembly", Journal of Manufacturing Science and Engineering, Vol.121, February 1999.

[36] Kolsky, H., "Stress Waves in Solids", Dover Publication, 1963.

[37] Timoshenko S. P. and Goodier J. N., "Theory of Elasticity", 3rd ed., McGraw-Hill.

[38] Johnson, W., "Impact Strength of Materials", Edward Arnold, London, 1972.

[39] Spotts, M. F., "Mechanical Design Analysis", Prentice-Hall, Inc., 1964.

[40] Macaulay, M. A., "Introduction to Impact Engineering", Chapman and Hall, 1987.

[41] Wada, Hiroshi "Reflection Characteristics of Longitudinal waves in a semi-infinite cylindrical rod connected to an elastic plate", Int'l J. Mech. Sci. Vol.26, No. 5, 1984.

[42] Boucher, S and Kolsky, H., "Reflection of the pulses at the interface between an elastic rod and an elastic half-space", J. Acoust. Soc. Am 52, p. 884, 1972.

[43] Burr, A. H., "Mechanical Analysis and Design", 2nd Edition, Prentice Hall, 1995.